STUDY ON SINGLE STRUT FORMATION USING ADDITIVE LAYER MANUFACTURING

CHEE YING CHEN

A thesis submitted
in fulfillment of the requirements for the degree of
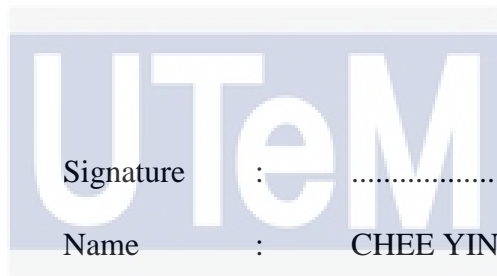**Bachelor of Mechanical Engineering (with Honours)**

Faculty of Mechanical Engineering

UNIVERSITI TEKNIKAL MALAYSIA MELAKA

2018

DECLARATION

I declare that this project report entitled "Study On Single Strut Formation Using Additive Layer Manufacturing" is the result of my own work except as cited in the references. The thesis has not been accepted for any degree and is not concurrently submitted in candidature of any other degree.

Signature : ....

Name : CHEE YING CHEN

Date : ....

ii

APPROVAL

I hereby declare that I have read this project report and in my opinion this report is sufficient in terms of scope and quality for the award of the Bachelor of Mechanical Engineering (with Honours).

Signature   : ....

Name of Supervisor   : DR RAFIDAH BINTI HASAN

Date   : ....

DEDICATION

I dedicate this thesis to my beloved mother and father; Chong Chuai Kuan and Chee Yok Choy who have always been giving me spiritual support while they are living at hometown, Cheras, Kuala Lumpur. I am truly appreciate their loves and patients when educating me from time to time. I also dedicate this thesis to all my siblings (Chee Ying Thung and Cheay Ying Wei) for being part of my life. My family has inspired me always and made me to be a better person in the future. Apart from that, I dedicate this thesis to my course mates and friends as they are willing to help whenever I have troubles in my life. They are rational to correct my mistakes and also give me some valuable advices.

ACKNOWLEDGEMENT

First and foremost, I would like to take this opportunity to express my deep appreciation to my supervisor Dr. Rafidah binti Hasan, from the Faculty of Mechanical Engineering Universiti Teknikal Malaysia Melaka (UTeM) for guiding me very well throughout this project. Under her supervision, I had gained her guidance and inspiration that enable me to complete this final year project successfully.

Moreover, I would like to express my greatest gratitude to Prof. Dr. Ghazali Bin Omar as my panel seminar and also second report examiner. Next, I would like to express my deepest gratitude to Associate Professor Dr Mohd Ahadlin bin Mohd Daud as my second panel seminar. He had lent the Dino-Lite Pro for me as well in order to complete the microscopic examination in this project.

Furthermore, I would like to thank to Universiti Teknikal Malaysia Melaka (UTeM) especially the Faculty of Mechanical Engineering (FKM) for giving a fully support by allowing me to use their equipments and facilities during conducting my project.

In addition, I would like to express my sincere thanks to my friends and course mates for giving me their supports and advices in this project. Next, special thanks to my parents and my siblings for giving me their loves, supports and encouragements throughout this project.

ABSTRACT

The lattice-structure materials are suitable for lightweight structural applications as they have the properties of flexible and high stiffness. In a lattice-structure material, its basic unit is single strut which is a member that connects two nodes. Hence, understanding the single strut properties is important in lattice-structure material study. This study is conducted to analyse layer by layer formation of fabricated single strut using a 3D printer with several parameters. The chosen diameters of single struts are 1.2mm, 1.4mm and 1.6mm while the build angles are set as 0°, 20°, 35.26^o, 45°, 60°, 80° and 90° from a vertical line. All single struts are needed to be designed with suitable supports before proceed to fabrication stage. After three sets of 21 specimens are fabricated using CubePro 3D printer successfully, all single struts are analysed on their diameter using Dino-Lite Pro. The difference between measured diameter and designed diameter for each single strut is recorded. Next, the selected single struts with 35.26^o build angle are analysed on their surface roughness using Dino-Lite Pro and 3D non-contact profilometer. A graph of surface roughness versus strut diameter is constructed for both equipment used. Thus, the results show that all single struts have the accuracy of more than 86% when comparing the readings of measured diameter and designed diameters. The single strut with 1.2mm diameter for 35.26^o build angles has the lowest R_a (Roughness Average) value. The comparison between individual strut and struts arranged in lattice structure in physical test is recommended to be conducted for future study.

ABSTRAK

Bahan struktur kekisi sesuai untuk aplikasi struktur ringan kerana mereka mempunyai sifat fleksibel dan kekakuan yang tinggi. Dalam struktur kekisi, unit asasnya ialah strut tunggal yang merupakan satu sambungan yang menghubungkan dua nod. Oleh itu, memahami sifat-sifat strut tunggal adalah penting dalam kajian bahan struktur kekisi. Kajian ini dijalankan untuk menganalisis lapisan pembentukan strut tunggal yang dibuat daripada pencetak 3D dengan beberapa parameter. Garis pusat yang ditentukan untuk strut tunggal adalah 1.2mm, 1.4mm, dan 1.6mm, manakala sudut membina ditetapkan sebagai 0°, 20°, 35.26^o, 45°, 60°, 80°, dan 90° dari garis menegak. Setiap strut tunggal diperlukan untuk direka dalam bentuk yang sesuai sebelum meneruskan ke peringkat fabrikasi. Setelah berjaya menghasilkan tiga set 21 spesimen dengan menggunakan pencetak 3D CubePro, semua strut tunggal dianalisis pada garis pusat dengan menggunakan Dino-Lite Pro. Perbezaan antara garis pusat yang diukur dan garis pusat yang ditetapkan untuk setiap strut tunggal juga dicatatkan. Seterusnya, strut tunggal dengan sudut 35.26^o yang dipilih dianalisis pada kekasaran permukaan mereka dengan menggunakan Dino-Lite Pro dan 3D non-contact profilometer. Graf kekasaran permukaan melawan saiz garis pusat strut ditunjukkan untuk kedua-dua peralatan yang digunakan. Oleh itu, keputusan menunjukkan bahawa semua strut tunggal mempunyai ketepatan melebihi 86% apabila membandingkan bacaan garis pusat yang diukur dan garis pusat yang ditentukan. Strut tunggal dengan garis pusat 1.2mm untuk 35.26^o sudut membina mempunyai nilai Ra (Purata Kekasaran) terendah. Perbandingan antara strut individu dan strut yang diatur dalam struktur kekisi dalam ujian fizikal adalah dicadangkan pada masa depan.

TABLE OF CONTENTS

LIST OF FIGURES

LIST OF FIGURES FOR APPENDICES

LIST OF TABLES

LIST OF ABBEREVATIONS

ABS   Acrylonitrile Butadiene Styrene

AM   Additive Manufacturing

Avg D   Average Diameter

BCC   Body Centered Cubic

CAD   Computer-Aided Design

CATIA   Computer Aided Three-dimensional Interactive Application

CO_2 Carbon Dioxide

EBM   Electron Beam Melting

FDM   Fused Deposition Modelling

PLA   PolyLactic Acid

R_a Roughness Average

SEM   Scanning Electron Microscope

SLM   Selective Laser Melting

STL   Standard Tessellation Language

LIST OF SYMBOL

n	=	Nodes
p	=	Struts
m_b	=	Mass of block
ρ_s	=	Density of the steel
L	=	Length of cell
N_1, N_2, N_3	=	Number of cells along the width, length and height directions
d	=	Strut diameter
x	=	Reading of measured diameter
N	=	Number of readings in a single strut
σ	=	Standard deviation
$\bar{x}$	=	Mean (average data)
x_e	=	Experimental value (measured diameter)
x_a	=	Actual value (designed diameter)
%	=	Percentage difference
l	=	Evaluation length
Z(x)	=	Profile height function

CHAPTER 1

INTRODUCTION

1.1   Background

Lattice-structure materials utilize the design principals of efficient, lightweight macroscale structures, to mesoscale material architectures. By having the properties of high stiffness and strength-to-weight scaling, the lattice-structure materials are suitable for lightweight structural applications. The basic unit of lattice-structure material is single strut. The assembly methods of the strut-based lattice structures are flexible because of the availability of the joint type. Hence, the complex geometries designs would prefer to apply the strut-based lattice structures due to its flexible configurations (Doyoyo and Hu, 2006).

For designing strut-based lattice structures, a lot of feasible options can be proposed within a defined volume as a lattice structure has variation number of nodes and struts. An example of lattice structure with its nodes (n) and struts (p) is shown in Figure 1.1. A node is a point where two or more struts join, while a strut is a connection or member that links two nodes (Syam et al., 2017).
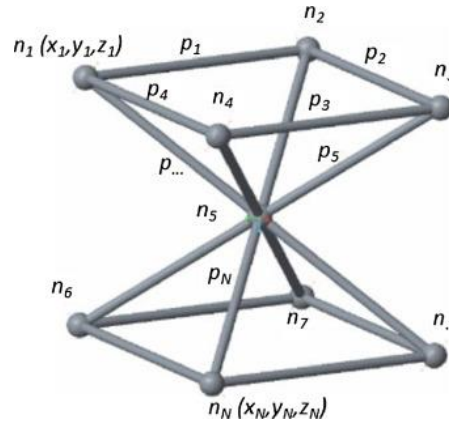
Figure 1.1: A strut-based lattice configuration with nodes n = 9 and struts p = 16.

(*Source: Syam et al., 2017*)

There are many methods in fabricating lattice-structure material, such as casting, sheet metal forming, wire bonding process, selective laser melting (SLM) and electron beam melting (EBM) (Rashed et al., 2016). Casting is one of the conventional methods to produce lattice structures by using injection molding and the mold is made by ceramic (Rashed et al., 2016). Sheet metal forming produces lattice structures by press forming operation from a roll of sheet metal (Rashed et al., 2016). SLM and EBM are both methods that using additive manufacturing (AM) techniques where the part is produced layer by layer. For SLM process, its raw material used is metal powder and the part is formed by depositing a thin powder layer and scanning by the laser (Gebhardt, 2003).

Additive layer manufacturing is an innovative method to fabricate lattice-structure materials. 3D printing is also an additive manufacturing (AM) which the printed part is formed layer by layer. By using AM technology, the design of lattice structure is needed to be drawn using a CAD software before proceed to printing machine. AM technology is an advanced method because it has high process flexibility and the possibility to produce parts with a high geometric complexity (Reinhart and Teufelhart, 2013).

2

1.2 Problem Statement

Understanding the single strut properties is important in lattice-structure material study. This is because, single strut is the basic unit of lattice-structure material. Different arrangement of struts can produce different architecture of lattice-structure material. Moreover, by producing lattice-structure material using additive layer manufacturing, many controlling parameters affect the properties of material. In this study, fabricated single struts using additive manufacturing are studied, in terms of its layer by layer formation. This is because there is no study done on investigating single strut using CubePro machine. Hence, the formation of single strut using material of polymer acrylonitrile butadiene styrene (ABS) and CubePro machine (Figure 1.2) will be examined at different diameter sizes and build angles.

Figure 1.2: CubePro machine at Rapid Prototyping Laboratory.

1.3   Objective

The objective of this study is to analyse layer by layer formation of fabricated single

strut using fused deposition modelling (FDM) machine with several parameters.

1.4   Scope of Project

The scopes of this project are:

1. To design single strut using CATIA (an acronym of computer aided three-
   dimensional interactive application) at different size and angles.

2. To fabricate single struts using CubePro 3D printer and material of polymer
   acrylonitrile butadiene styrene (ABS).

3. To evaluate the formation of single strut and relate it with process parameters
   using microscopic examination, which is optical microscope and profilometer.

1.5   Summary of Chapter 1

In conclusion, the fabricated single struts using additive manufacturing are studied in

order to quantify the single strut as a basic unit of lattice structure. By conducting this study, the

formation of single strut with different diameter sizes and build angles can be evaluated. The

next chapter will describe about the literature review of this study.

CHAPTER 2

LITERATURE REVIEW

2.1   Introduction

The background of this study is needed to be studied in order to have better understanding before proceed for further progress. In this chapter, the relevant topics with this study are explained based on the journal articles and academic book. Moreover, the researches that related to this study are discovered from the journal articles and described in this chapter as well.

2.2   Lattice-structure and Strut

Lattice-structure is formed by a number of struts and nodes. Node is a joint where struts meet together while strut is the basic unit of lattice structure and also as a connection between nodes. For designing strut-based lattice structure, it can be designed in various types of configuration due to the variation of node positions in a fixed volume. Lattice-structure has high stiffness-to-weight ratio, which means its materials used can be saved. Hence, the strut-based lattice structures are being applied in complex geometries designs as the problem of forming can be eliminated (Doyoyo and Hu, 2006).

There is a large number for the formation of strut-based lattice structure that can be designed within a fixed volume when the number of nodes and struts are not fixed. Since the

variation of the number of nodes and struts can lead to obtain a large number of options results, the node positions and strut diameters can be variable in a specific volume as well (Syam et al., 2017). Strut-based lattice structure can be in various shape such as cubic truss and octetruss as shown in Figure 2.2.
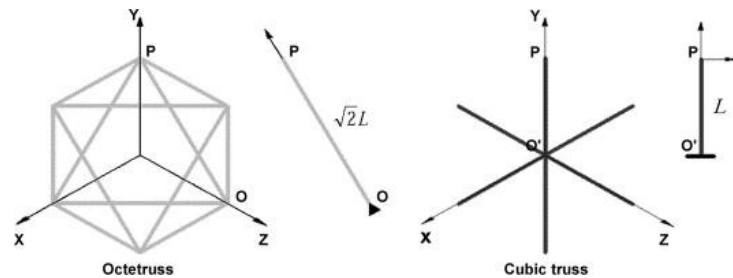

Figure 2.2: Octetruss and cubic truss.

(Source: Doyoyo and Hu, 2006)

2.3   Methods in Producing Lattice-structures

Traditionally, lattice-structures are manufactured through casting, sheet metal forming, or wire bonding processes. These conventional manufacturing processes are time-consuming and also limited the complexity of lattice-structure designs. These methods are only used to manufacture lattice-structure materials with simple configuration on a macroscale (Tang et al., 2017).

For casting process, a pattern of wax or polymer lattice-structure is coated with ceramic casting slurry. This ceramic is a mold and the wax or polymer is then removed through the process of melting. The liquid metal with high fluidity can be used to fill in the empty mold in order to form lattice-structure material. By using this method, a wide range of shapes of lattice structure can be formed as it depends on the shape of the mold that can be designed to be desired

6

shape. Figure 2.3.1 shows octet-truss lattice structure produced from casting process. With this casting process, the manufactured lattice-structure material had severe porosity and this method is expensive and time-consuming (Rashed et al., 2016).
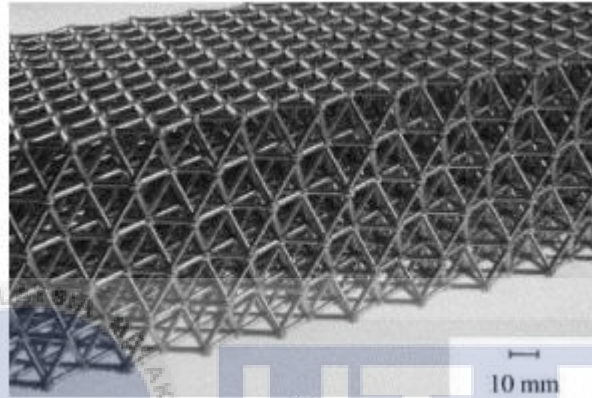

Figure 2.3.1: Octet-truss lattice structure.

(Source: Rashed et al., 2016)

For sheet metal forming method, a roll of sheet metal is went through perforation punch to form the shaped holes such as hexagonal or diamond. The elongated perforated sheet is treated with annealing process to soften the struts before proceed to punching process. The perforated sheet is then bent by the combinations of punch and die. This punching process allows the perforated sheet to be corrugated. Hence, a simple lattice-structure material can be manufactured through these processes from a sheet metal. Figure 2.3.2 shows the processes of sheet metal forming method (Rashed et al., 2016).
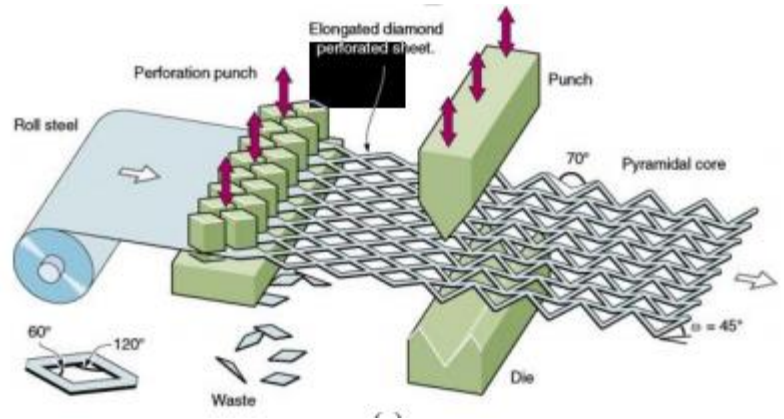
Figure 2.3.2: Sheet metal forming process.

(Source: Rashed et al., 2016)

However, the introduction of additive manufacturing (AM) technologies had reduced the limitations in producing lattice-structure materials. AM technologies manufacture a part layer by layer and enables the design of lattice-structure materials in complex configuration. A complex lattice-structure can be produced in ease through AM technologies and also in variation of geometrical scales such as microscale, mesoscale or macroscale (Reinhart et al., 2012).

2.4   Additive Layer Manufacturing

Generally, the first process of AM technology is to design and build a 3D modeling using a CAD (Computer-Aided Design) software. This drawing is later converted into a "STL" (Standard Tessellation Language) file format which originates from 3D Systems. A computer program can read the STL file to create slices from the model for data preparation. This data is inserted into a program of an AM machine for producing the designed parts. Post processing is needed to carry out for removing support structure or surface finishing (Kessler et al., 2016).

8

3D printing is one of the additive layer manufacturing technologies. There are different types of 3D printing and can be classified by depending on the raw materials such as solid-based, liquid based or powder based (Gebhardt, 2003). A lattice-structure material or single strut can be fabricated by using 3D printing which is done within one process only where the part is generated layer-by-layer (Kessler et al., 2016).

There was a study on producing strut shape of lattice-structure using SLM (Selective Laser Melting) method. It was a powder-based AM technology and its raw material used was metal powder. During SLM process, a thin powder layer was deposited, and CO_2 (carbon dioxide) laser was irradiated to the powder surface successively until final part was produced based on CAD data. It focused on few types of cross sectional shape of struts and its reached quality. The examined shapes were circular, elliptical, square, triangular and rhombus. By producing these struts, the limitations of SLM process were evaluated. For example, the limitation for circular cross section was the nominal diameter which smaller than 0.15mm cannot be fabricated (Kessler et al., 2016). Figure 2.4 shows the fabricated struts with different diameters.

Figure 2.4: Fabricated struts with different diameters.

(Source: Kessler et al., 2016*)*

There was another study about stainless steel micro-lattice block structures that were produced using SLM process. An equation was derived to estimate the strut diameter in a Body Centered Cubic (BCC) micro-lattice block structures made by stainless steel in SLM process. This equation is as stated in Equation 3.1. From Equation 3.1, m_b is the mass of block, ρ_s is the density of the steel, L is the length of cell, the N_1, N_2, N_3 are the number of cells along the width, length and height directions. This equation was used to calculate the strut diameter of fabricated micro-lattice block structures with different SLM process parameters (Tsopanos et al., 2016).

$$d = \sqrt{\frac{m_b}{\rho_s \,.\pi\,.N_1 \times N_2 \times N_3 .L\,.\sqrt{3}}} \qquad [3.1]$$

2.5   Polymer 3D Printer

In this study, strut formations are fabricated by polymer 3D printer and it uses FDM (Fused Deposition Modeling) method. The plastic material in filament form is melted and the semi-liquid material is extruded. The extruded material is then solidified to form the model. This formation is built layer-by-layer. There are some parameters that can affect the performance and functionalities of the system, such as material strength, deposition speed, layer thickness and envelope temperature (3dsystems, 2017).

The 3D printer chosen for this study is CubePro Printer. It has the features of ultra-high-resolution setting of 70 microns, 200 microns and 300 microns thin print layers. It has also Z axis resolution of 0.1mm which means it has good accuracy in printing the model. The deposition speed can up maximum 15mm per second and the maximum operating temperature at extruder tip is 280°C. The materials used for this printer is PLA (polylactic acid) or ABS

(acrylonitrile butadiene styrene) (3dsystems, 2017). Figure 2.5 shows a CubePro Printer that used to print the strut formations.

Figure 2.5: CubePro 3D printer.

2.6   Summary of Chapter 2

In conclusion, knowledge is gained through reviewing the background of this study from the relevant journal articles and book. The relevant scientific theories are learnt from the researches such as the limitations of SLM process in producing these struts and the equation which can estimate the strut diameter. After understanding the background of this study, the methodology for conducting this study is planned and described in the next chapter.

CHAPTER 3

METHODOLOGY

3.1   Introduction

In conducting this study, a workflow is decided and presented in this chapter. This study is carried out through a series of processes. The first process is design of single struts, next process is fabrication of single struts and the last process is the analysis of printed single struts. The description of each process is explained in details in this chapter.

3.2   Workflow Chart

The actions that needed to be carried out for conducting this study are listed as below. Figure 3.2 presents the flow chart of methodology in this study. Firstly, literature studies are conducted from the relevant journals, articles or any materials to review 3D printing and single strut. Next, single struts are designed and drawn with different diameter sizes and build angles using a computer-aided design (CAD) software such as CATIA. In fabrication stage, the designed single struts are printed using a 3D printer which is the CubePro machine. After the single struts are fabricated successfully, these single struts are evaluated on their diameters and surface roughness using a portable optical microscope which is Dino-Lite Pro. Lastly, a report on this study will be written at the end of the study. At the end of FYP I, the preliminary results

are obtained at the fabrication stage. In this FYP II, all single struts should be confirmed to be

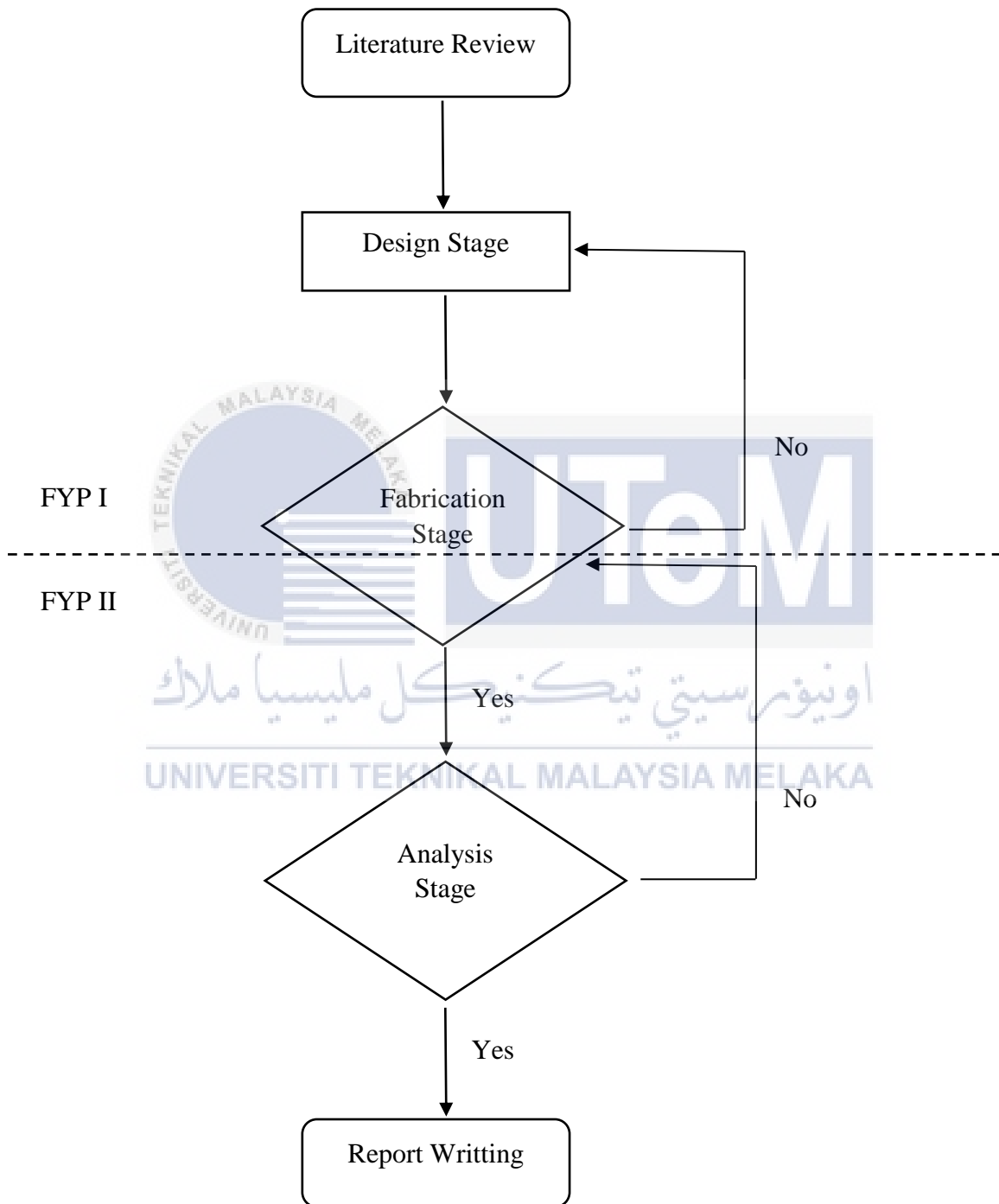printed successfully based on their designs before proceed to analysis stage.

Figure 3.2: Flow chart of the methodology.

3.3   Design Stage

Table 3.3: Parameters of single struts.

Diameter (mm)	1.2	1.4	1.6
	0	0	0
	20	20	20
	35.26	35.26	35.26
Build angle from vertical (º)	45	45	45
	60	60	60
	80	80	80
	90	90	90

The parameters of the single struts are set to have three different diameters which are 1.2mm, 1.4mm and 1.6mm as shown in Table 3.3. The 1.2mm diameter is chosen as the smallest diameter to be fabricated as the CubePro printer is able to print strut with at least 1.0 mm diameter (Azmi et al., 2017). The build angles for the single struts are 0º, 20º, 35.26º, 45º, 60º, 80º and 90º from a vertical line. The 35.26º is chosen as it represents the angle of the strut to the surface in BCC structure. There are 21 specimens to be produced to study their potential to be fabricated.

These 21 single struts are designed and drawn using a CAD software which is CATIA. An example of a part drawing and a dimension drawing of the single struts are shown in Figure 3.3.1 and 3.3.2 respectively. The side support for each single strut is designed to ensure the strut can be printed successfully. After the designed 3D modelling of these single struts are selected, this drawing is then converted in to "STL" (Standard Tessellation Language) file format in CATIA software. This STL file is then transferred to the software of CubePro to create slices from the model of single struts for data preparation before producing the single struts.
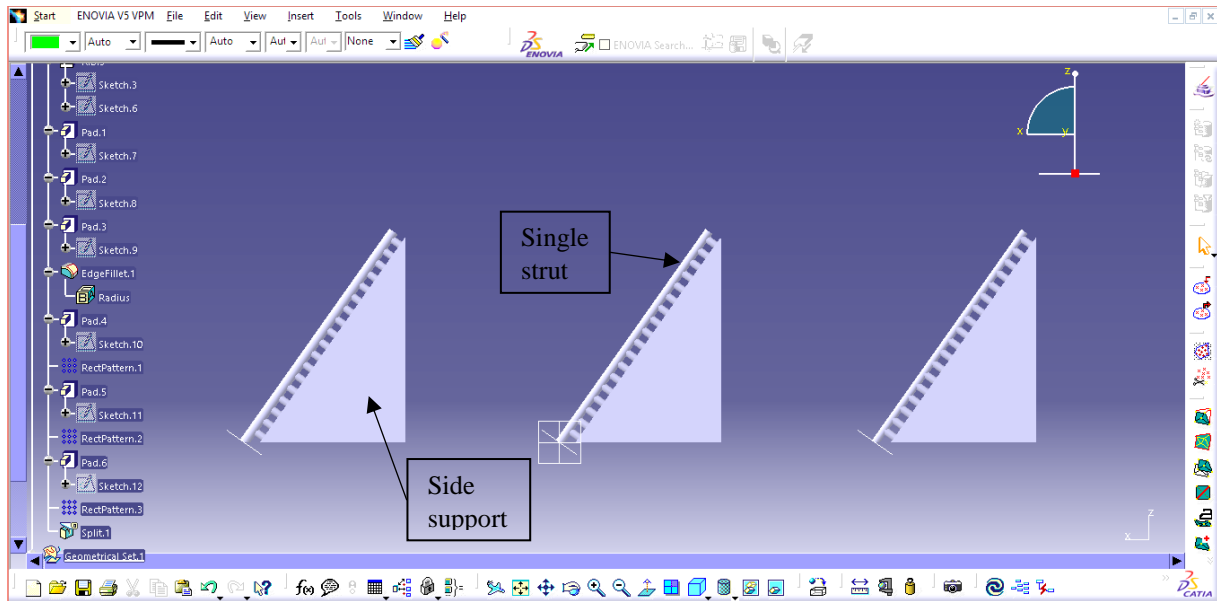
14

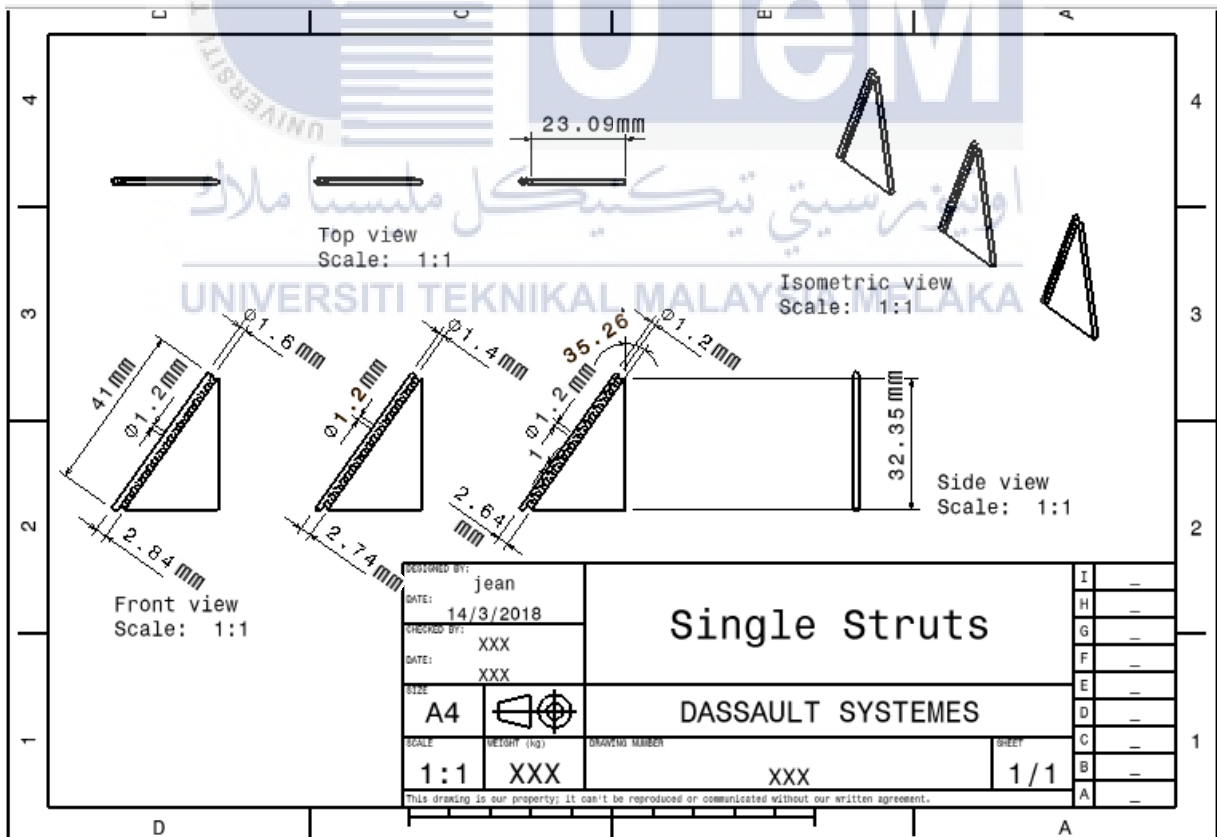Figure 3.3.1: The part drawing of single struts with 35.26º using CATIA.

Figure 3.3.2: The dimension drawing of single struts with 35.26º using CATIA.

3.4 Fabrication Stage

Once the selected STL file is opened in the software of CubePro, there is a build setting to create slices of the model of single struts for being built layer by layer during later 3D printing process. From the build settings, several process parameters can be chosen for printing the designed part. Figure 3.3.1 and 3.3.2 show the build settings and their descriptions of CubePro software. In the software, the bottom supports of single struts are generated by itself as shown in Figure 3.4.3.
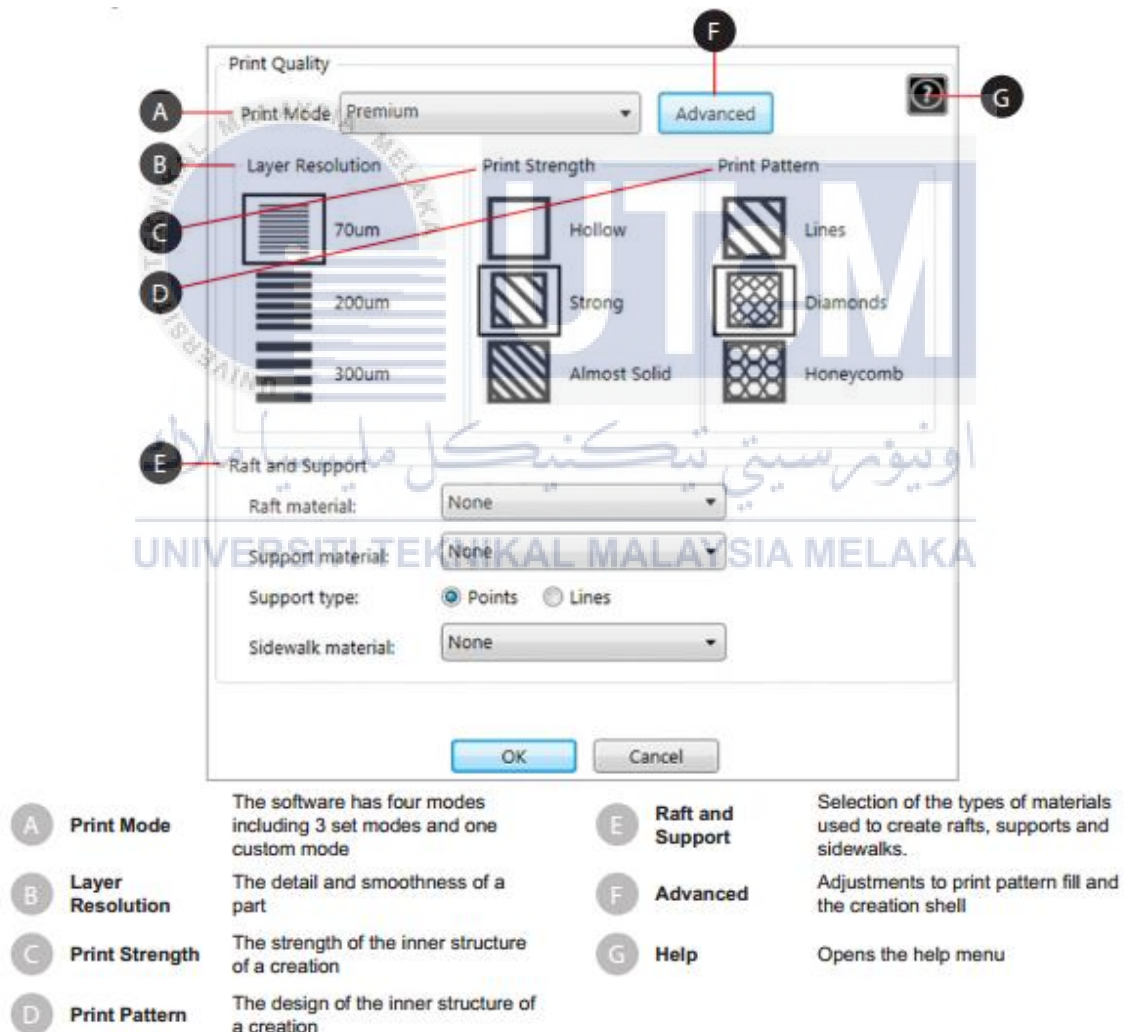
Figure 3.4.1: Build settings of CubePro software.

(Source: 3D Systems Inc., 2015)

Print Mode			
	Standard	•	Layer Resolution: 200um
		•	Print Strength: Strong
		•	Print Pattern: Diamonds
	Premium	•	Layer Resolution: 70um
		•	Print Strength: Strong
		•	Print Pattern: Diamonds
	Draft	•	Layer Resolution: 300um
		•	Print Strength: Strong
		•	Print Pattern: Lines
	Custom		Custom allows the user to customize their print settings
Print Resolution			
	0.070	•	Great mode for parts requiring smooth surfaces
		•	Layer lines are not very visible in these parts
		•	Good mode for artistic parts with a smooth flow
		•	Not the best mode for fine detail
	0.200	•	Best mode for general printing and most compatible mode for a wide range of geometries
		•	Fine detail preservation for things like steeples, spires, sharp points, or thin walls
	0.300	•	A fast mode with thicker layers
		•	Good for large parts with minimal detail
Print Strength			
	Hollow	•	Fastest mode to produce a part
		•	Hollow has fewer outer surfaces and larger print pattern spacing
		•	Best for parts that will not be stressed
	Strong	•	Medium amount of outer surfaces and smaller print pattern spacing
		•	Best for parts that will have minimal physical abuse
	Almost Solid	•	The most surfaces and the tightest print pattern spacing
		•	The most robust part
		•	Best for parts that will be stressed
Print Pattern			
	Lines	•	Fastest print fill pattern
		•	Minimal cross bracing
	Diamonds	•	Strong print pattern with 2-direction cross bracing
	Honeycomb	•	Strong print pattern with 3-direction cross bracing

Figure 3.4.2: Descriptions on the build settings.
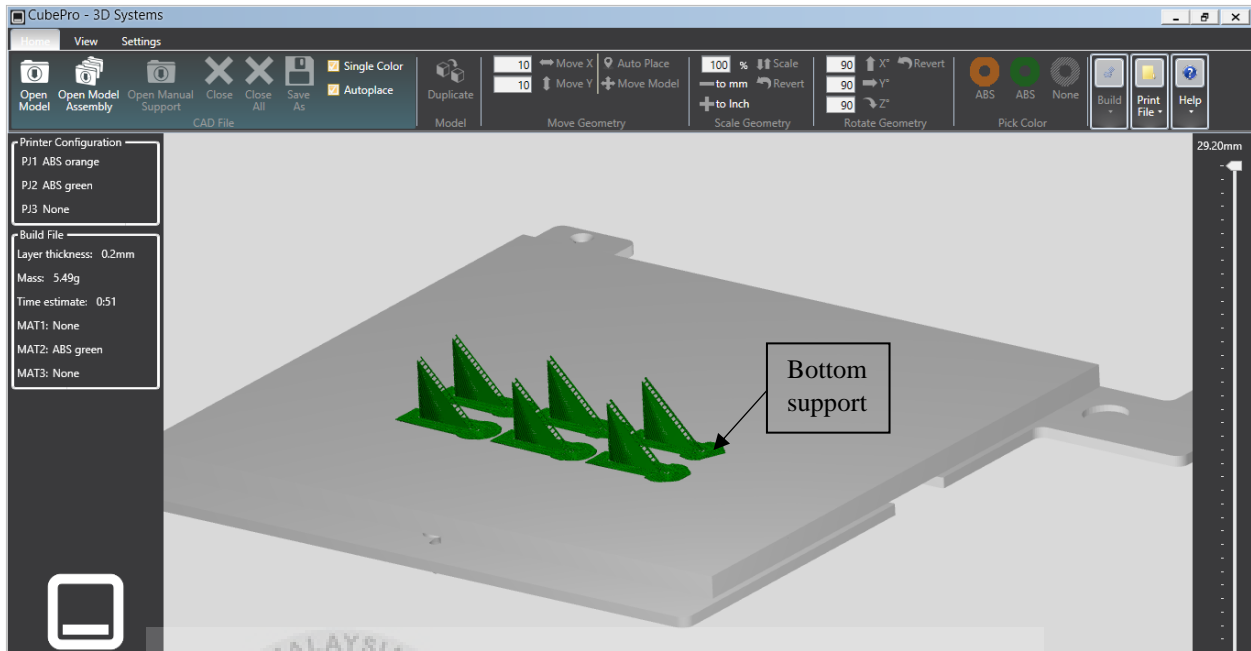
(Source: 3D Systems Inc., 2015)

Figure 3.4.3: Single struts with slices in CubePro software.

Table 3.4.1: Process parameters selected for single struts.

Strut Diameter (mm)	Layer Resolution (µm)	Print Strength	Print Pattern
1.2	200	Solid	Cross
1.4	200	Solid	Cross
1.6	200	Solid	Cross

For the formation of the single struts in this study, the process parameters are selected

as shown in Table 3.4.1. By referring to description in Figure 3.4.2, the 200 µm layer resolution

is chosen because it is suitable for wide range of parameters, and the solid is the strongest form

to be printed. After the selections of the build settings, the Cube Glue is needed to apply on the

platform of the printing bed. The glue can prevent the printed part from moving during the

printing process. The heating process is then began to heat up the nozzle and also the printing bed. When the nozzle and the printing bed are heated to the predetermined temperature, the printing process is started. The temperature of the nozzle is just below the melting point of the ABS material used because the materials is extruded in molten form during printing process. Figure 3.4.4 shows the printing process of struts using CubePro 3D printer. Hence, three sets of single strut specimens are fabricated in this study and several single struts are printed at once to reduce the time taken for printing.

Figure 3.4.4: Printing process of struts using CubePro 3D printer.

3.5   Analysis Stage

Before proceed to the analysis stage, there is a need to separate the single strut and its built supports. The bottom support can be detached easily by hand as shown in Figure 3.5.1. This is because it is so flimsy and also auto-generated by Cube Pro software. Next, the side bottom is cut off using a trimming knife as shown in Figure 3.5.2. Therefore, it is easier to cut the tiny supports later. Moreover, the tiny supports are cut by a trimming scissor as shown in Figure 3.5.3. This cutting process must be done carefully to ensure the single strut is not damaged. Lastly, each single strut is labelled by its diameter and build angle using masking tape and a marker pen as shown in Figure 3.5.4 (a) and (b) for recognizing them easily. Figure 3.5.5 shows the completed three sets of printed single struts.
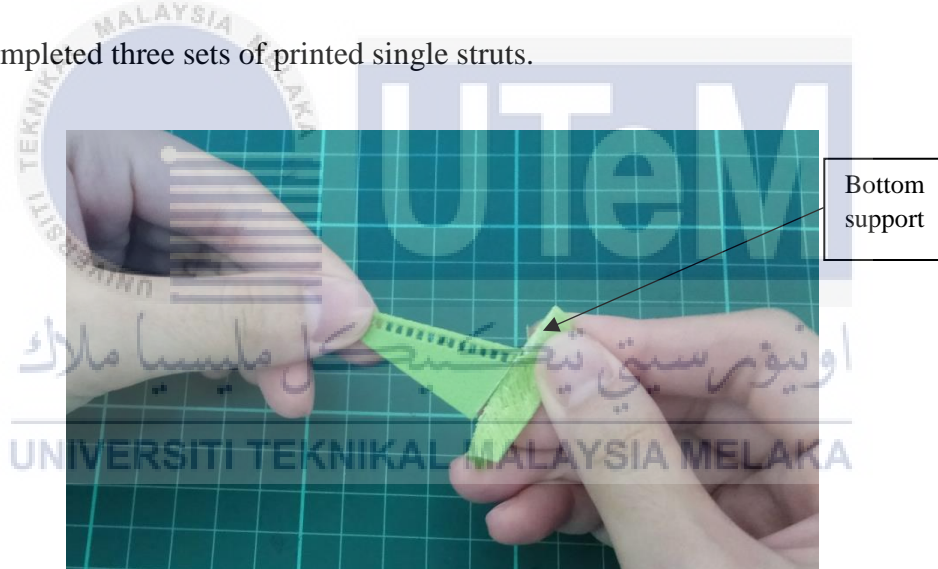
Figure 3.5.1: Detach the bottom support.
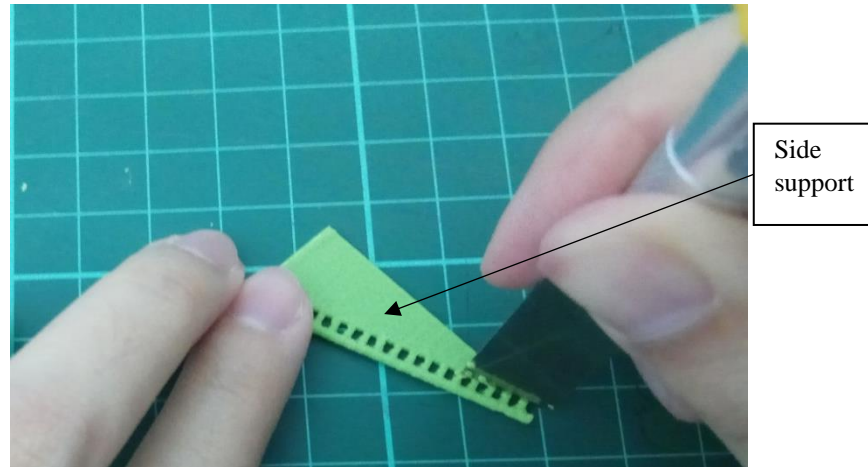
Side
support

Figure 3.5.2: Cut off the side bottom.
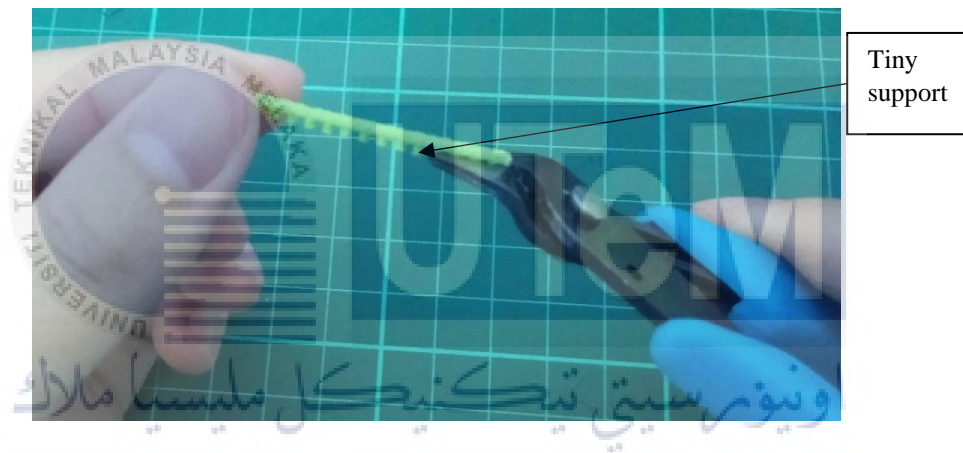
Tiny
support

Figure 3.5.3: Tiny supports are cut.
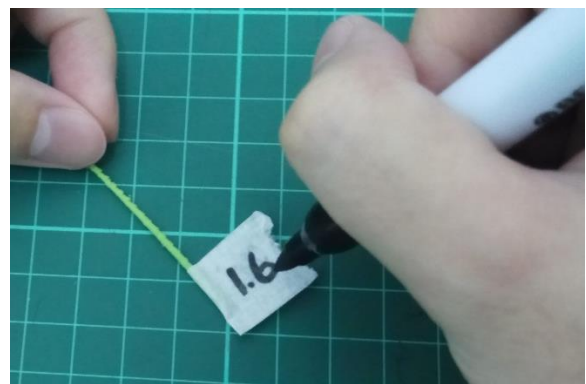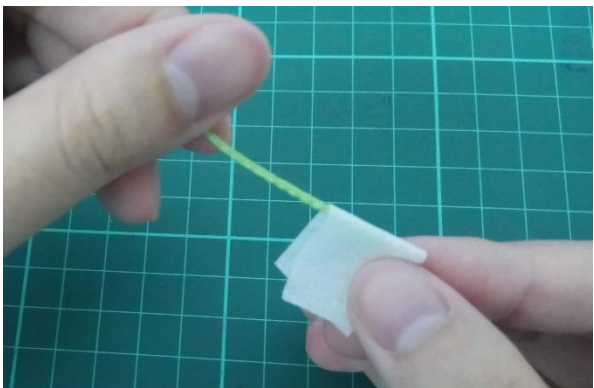
Figure 3.5.4: Single strut is labelled using (a) masking tape and (b) a marker pen.

21
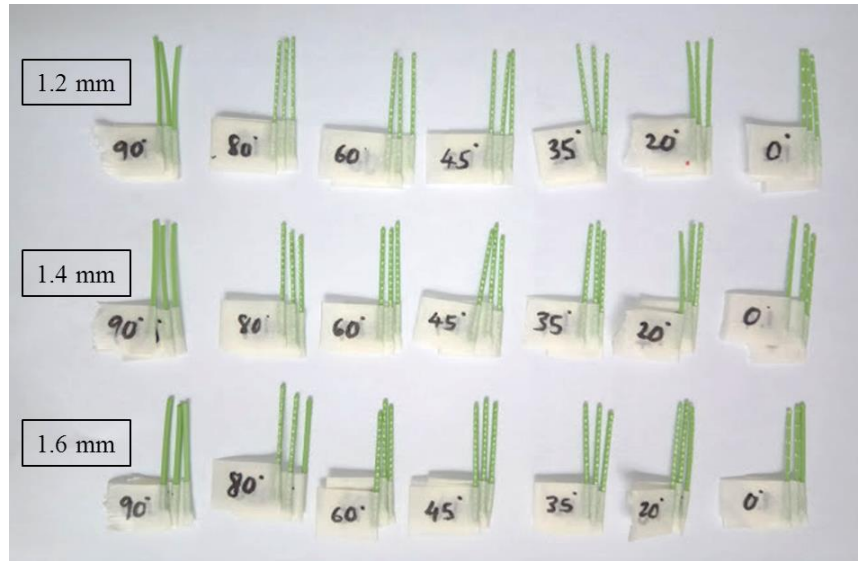
Figure 3.5.5: Three sets of printed single struts.

When all single struts have been separated, the microscopic examination is carried out by using a portable optical microscope for the analysis. The equipment chosen is called Dino-Lite Pro and it has variable magnification from 10x up to 220x as well. This Dino-Lite Pro includes its software for computer in order to capture image and measuring purposes. When this Dino-Lite Pro is connected with a computer, a single strut is placed under the microscope with its stand as shown in Figure 3.5.6. By having this advanced optical microscope, a clear image of single strut can be observed and the diameter of single strut can be measured. Apart from that, the surface roughness also can be analysed by measuring several peak values and also valley values on the selected single struts.
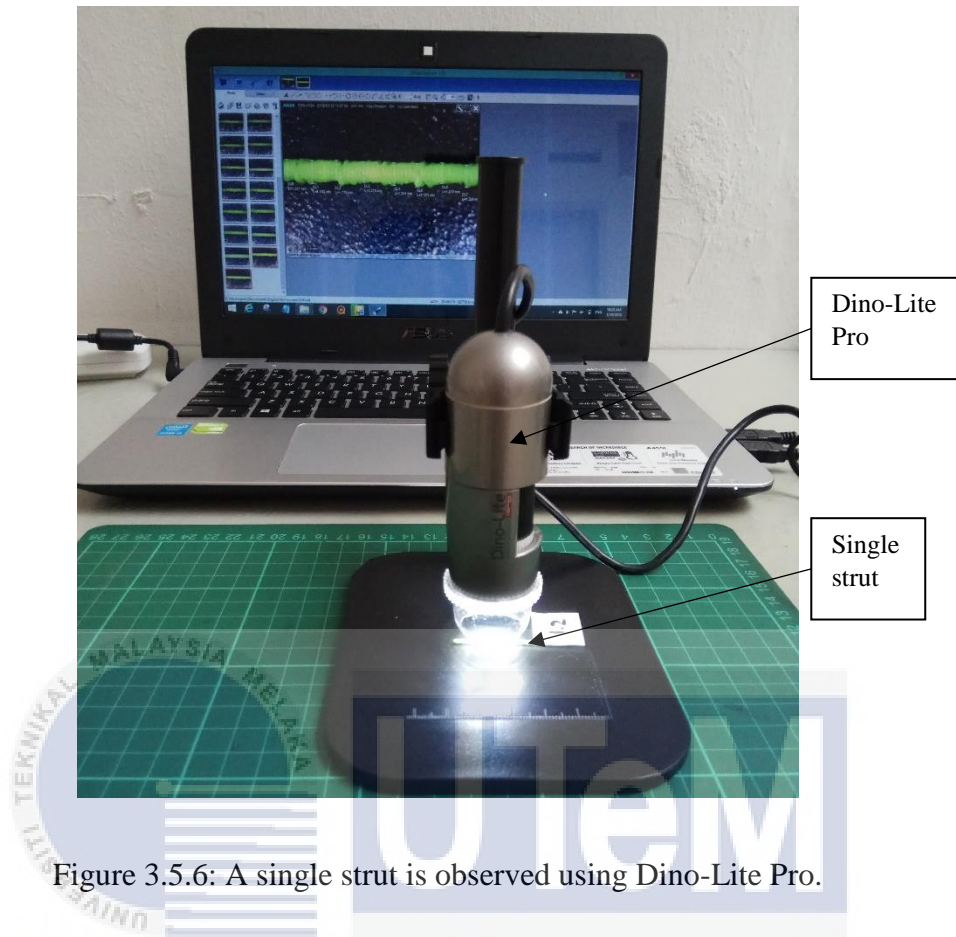
Figure 3.5.6: A single strut is observed using Dino-Lite Pro.

Another equipment that used to measure the surface roughness is 3D non-contact profilometer as shown in Figure 3.5.7. By placing the specimen under the mocroscope, the image can be clearly seen and captured in its software called WinRoof. Next, from the image showed in the software, the examined specimen can be viewed so that the roughness value can be obtained through scanning its surface. The results obtained from the software can be exported and saved in a Excel file.
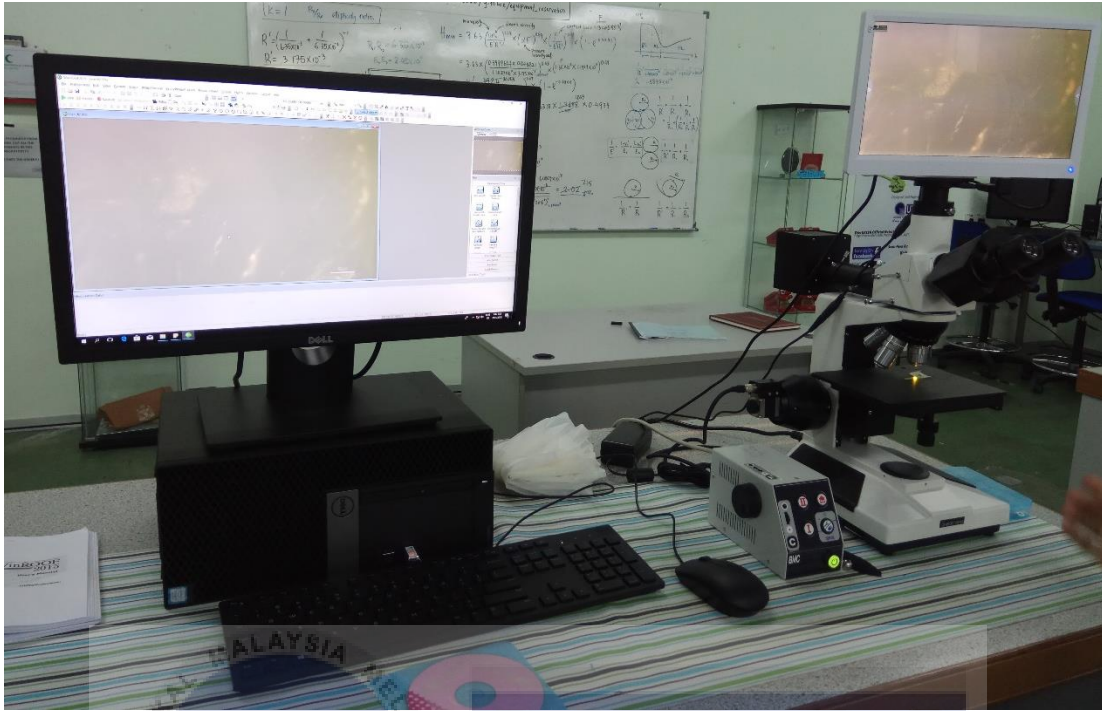
Figure 3.5.7: 3D non-contact profilometer.

3.6   Summary of Chapter 3

In conclusion, methodology is the plan to figure out all activities to be done in this study. In fulfilling this study, the strategy is arranged well so that these activities can be conducted according to the plan. Hence, the results are obtained from this study and discussed in the next chapter.

CHAPTER 4

RESULTS AND DISCUSSION

4.1 Introduction

The results that have obtained for this study are discussed in this chapter. These results are obtained from the three different stages, which are design stage, fabrication stage and analysis stage. At each stage, the results obtained are discussed and explained clearly before making a conclusion.

4.2 Design Stage

From the results obtained in PSM I, the bottom supports are automatically generated for all single struts as shown in Figure 4.2.1. Apart from that, the struts with 60º and 80º have their own side supports because their overhang angles are 30º and 10º respectively. Since their overhang angles are less than 35º as shown in Figure 4.2.2, the side supports are automatically generated as it is originally set in the program of CubePro as shown in Figure 4.2.3. However, some of the single struts are not fully printed and hence the decision is made for subsequent printing process where the single struts are printed separately.
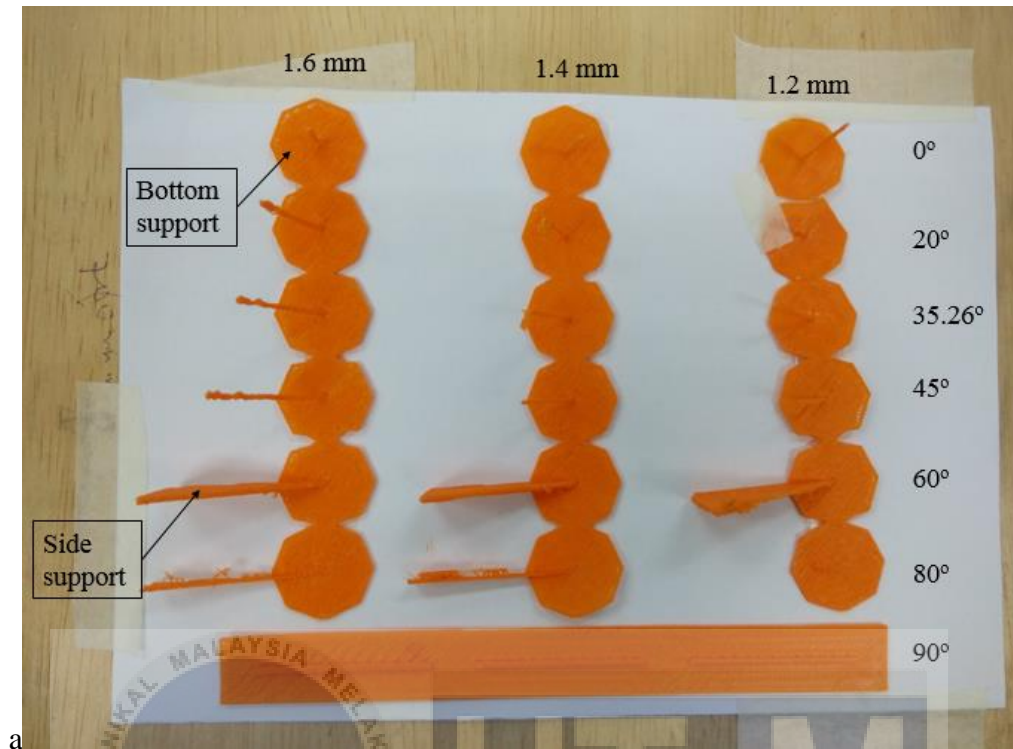
Figure 4.2.1: Top view for printed single struts using CubePro 3D printer.
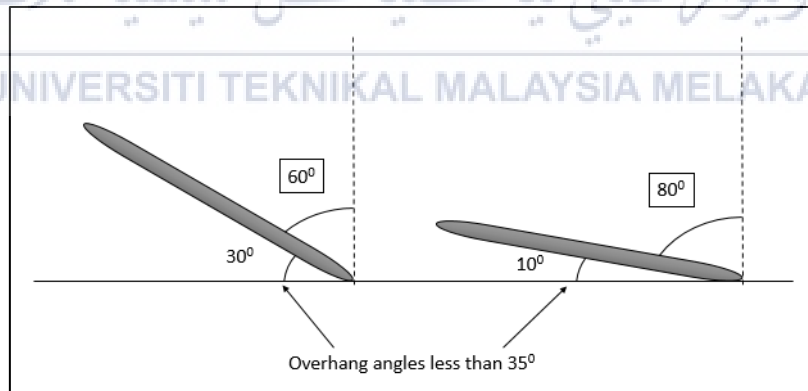
Figure 4.2.2: Schematic diagram of overhang strut angles.
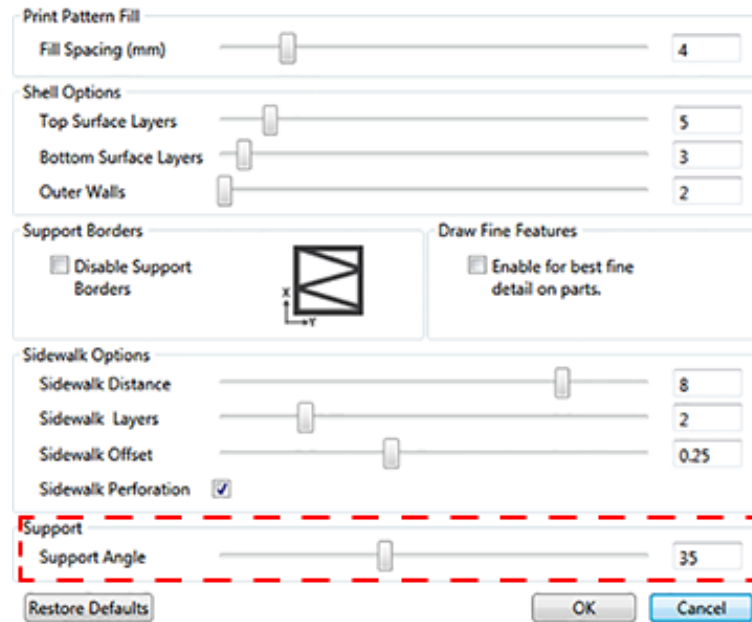
Figure 4.2.3: Support angle setting.

(Source: 3D Systems Inc., 2015)

In this design stage of PSM II, some feasibility tests are carried out before printing all the single struts. This process is to find out the weakness of the design and then to improve the design. Hence, this process can ensure the single struts are printed successfully. Figure 4.2.4 shows the failures of specimens during the experimental tests. Based on feasibility tests, each single strut should have its suitable support and therefore the side support is designed for each single strut. After the designs of all single struts are completed, the single struts are arranged well and to be printed using CubePro 3D printer. As the single struts are confirmed to be printed successfully, several single struts are then be printed together at once. Figure 4.2.5 shows an example of printed single struts on the printing bed. By printing several single struts together at once, it has enhanced printing efficiency as it can save times as compared to printing single struts separately for many times.

27

Too rough at the end

Tiny supports and strut are not printed well

Some part is over hang, tiny supports are not enough
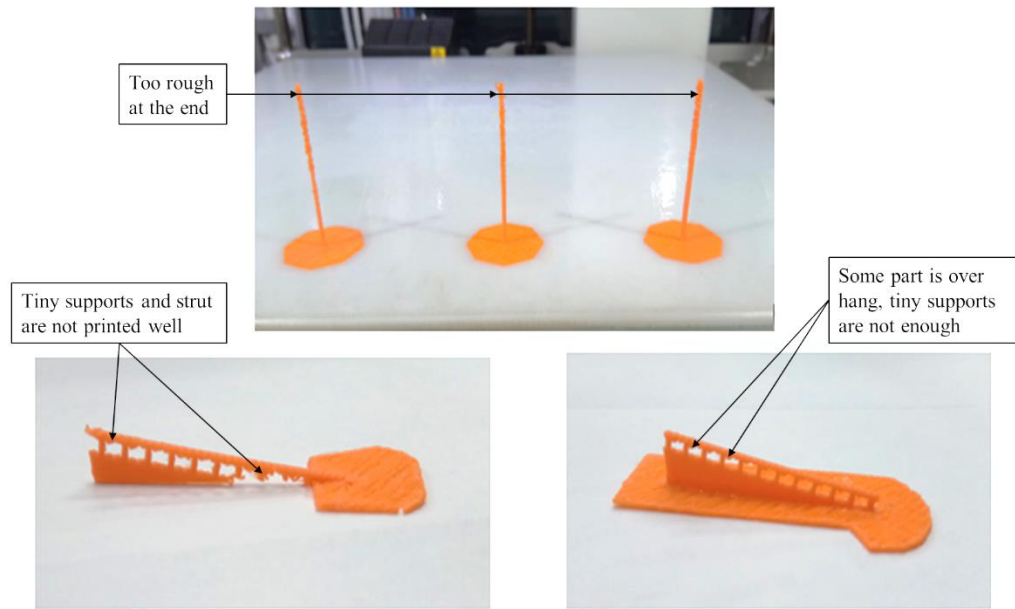
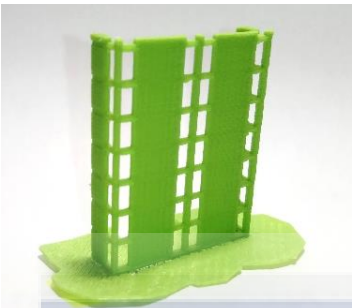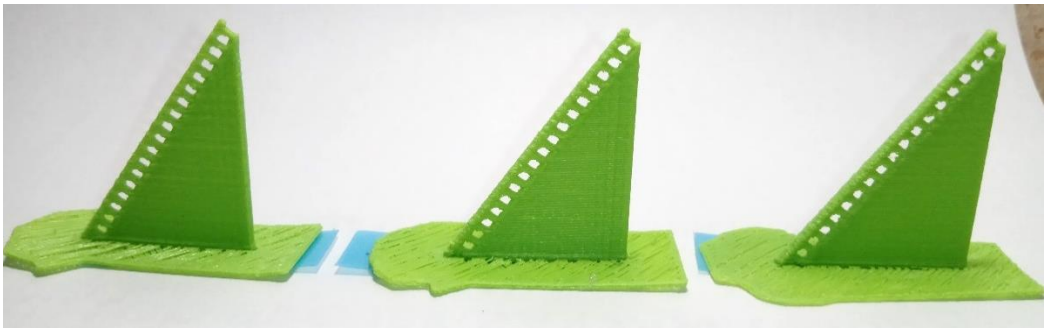Figure 4.2.4: Specimens from feasibility tests.
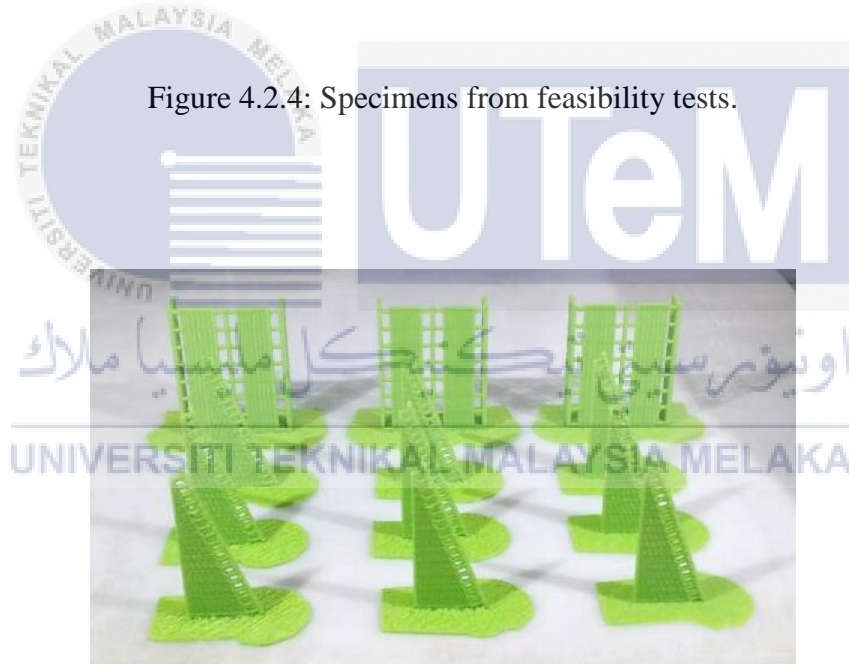
Figure 4.2.5: Several printed single struts on the printing bed.

4.3   Fabrication Stage

Table 4.3: A set of successfully printed specimens.

Build angle (°)	Struts		
	Diameter, d (1.2mm)	Diameter, d (1.4mm)	Diameter, d (1.6mm)
0			
20			
35.26			
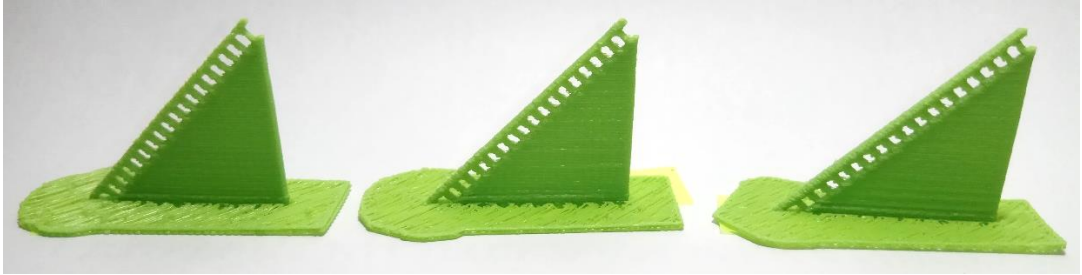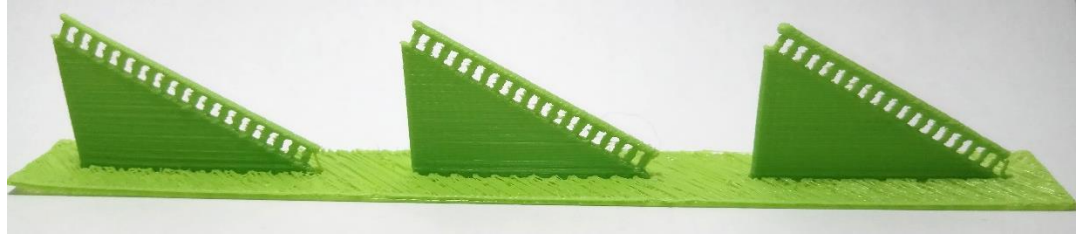
45	
60	
80	
90	

Table 4.3 shows a set of single struts which are printed successfully from CubePro 3D printer. Single struts with 0° build angle have the different designed support with others as they are printed straight upward. On the other hand, single struts with 90° build angle do not have any support as they are printed by laying on the printing bed as well.

4.4   Analysis Stage

For the analysis process, each single strut is observed under the portable optical microscope, called as Dino-Lite Pro. The no trimming surface of single strut is chosen for this observation because to avoid the trimmed surface affect the diameter readings as shown in Figure 4.4.1 (a) and (b). Moreover, the formation of each single strut is clearly seen using the software, which is layer-by-layer. The magnification scale of 45x is used throughout this observation process for all single struts as shown in Figure 4.4.2. Next, eight points are selected to measure the diameter on the selected single strut. The average readings of the measured diameter for each single strut are recorded in the Table 4.4.1.

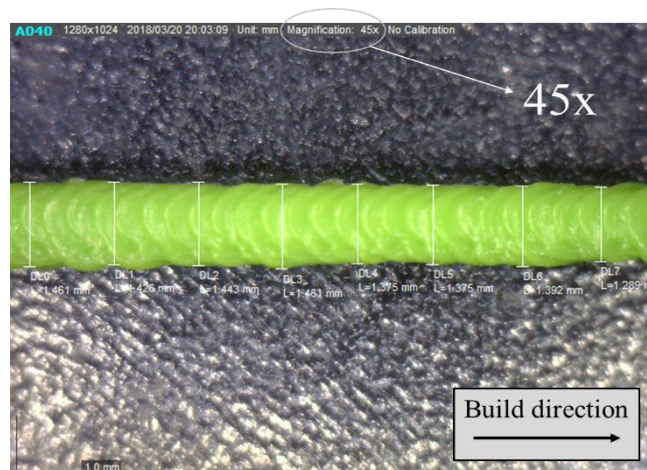Figure 4.4.1: (a) Surface with no trimming and (b) trimmed surface of single strut.
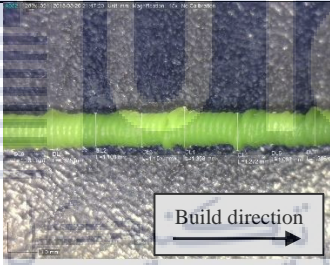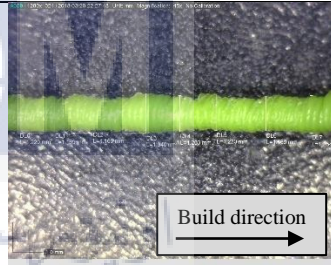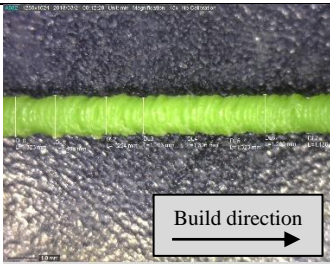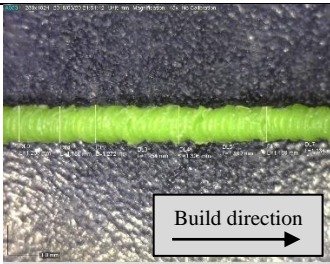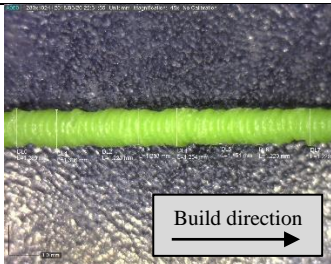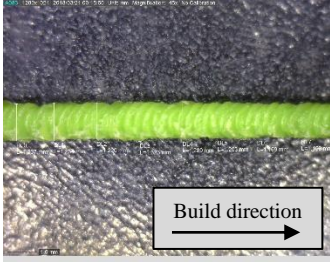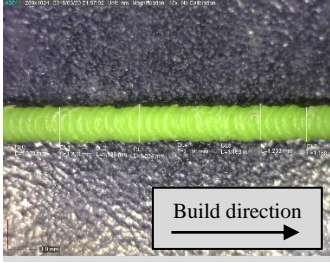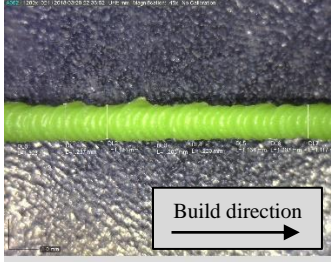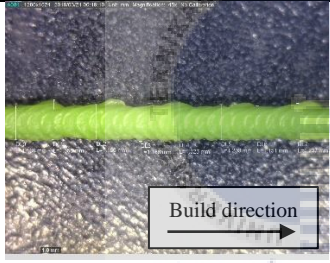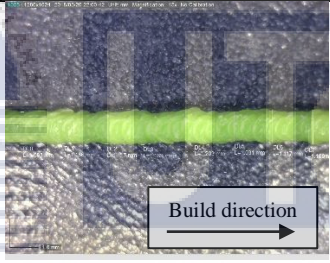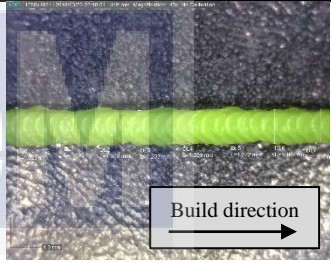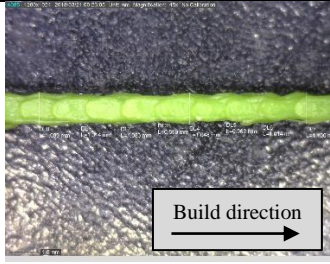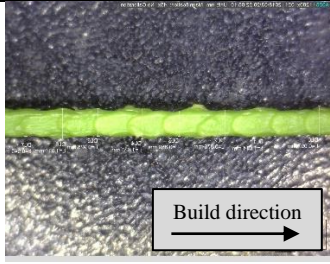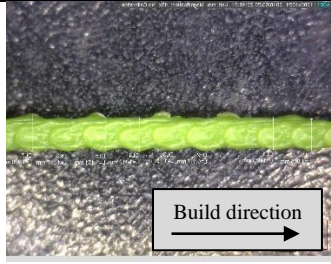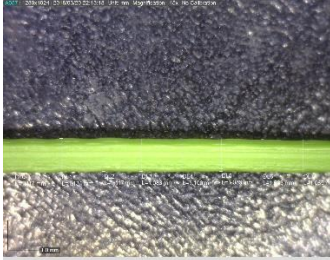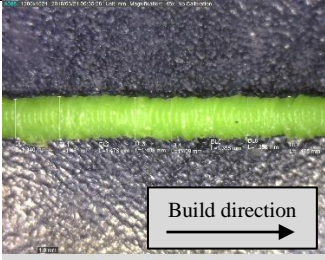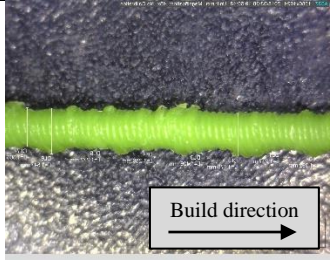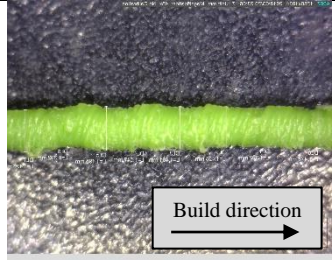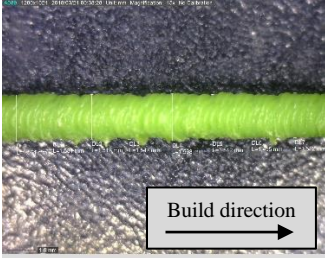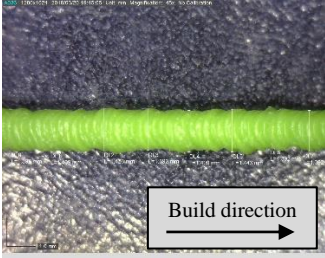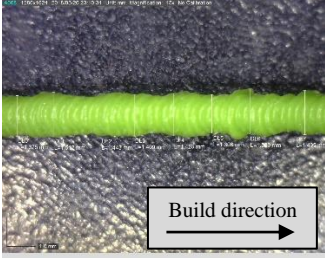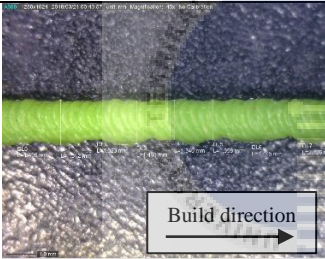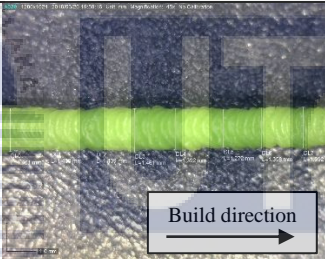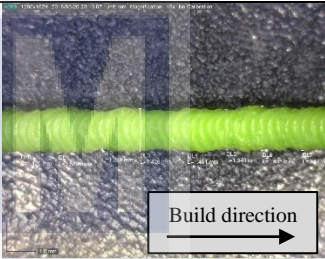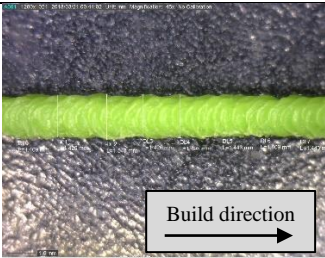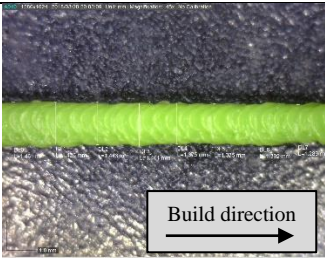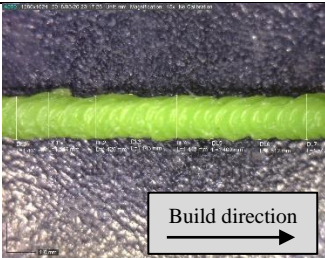
Figure 4.4.2: Magnification scale used in Dino-Lite software.
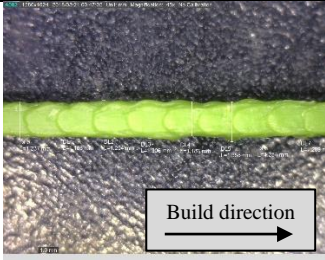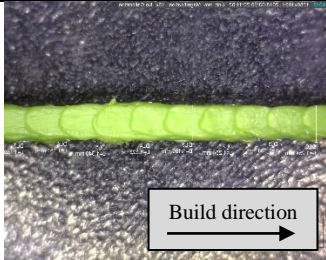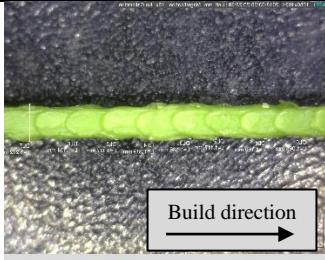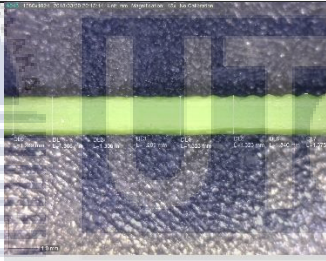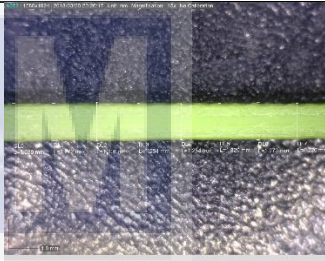
Table 4.4.1: The readings of the measured diameter for each single strut.
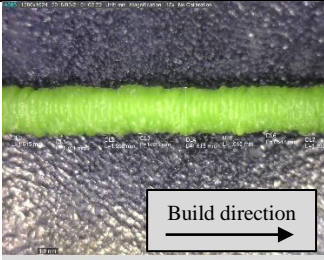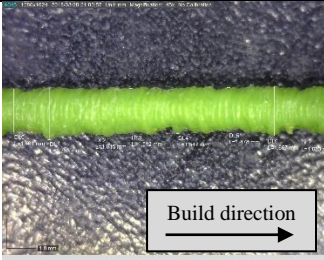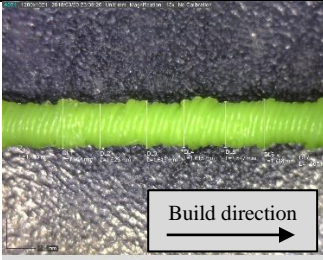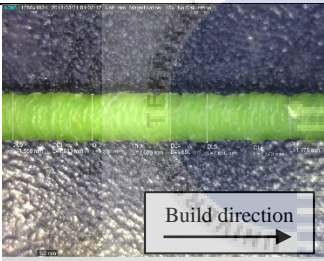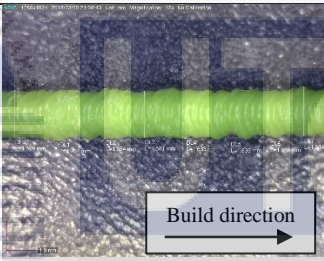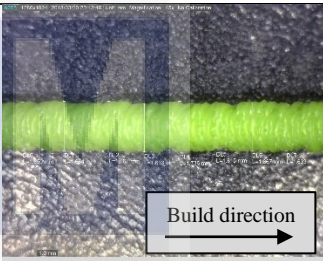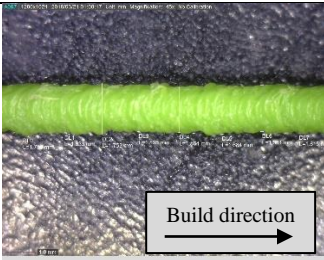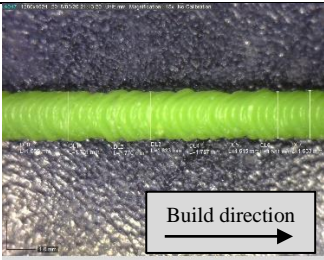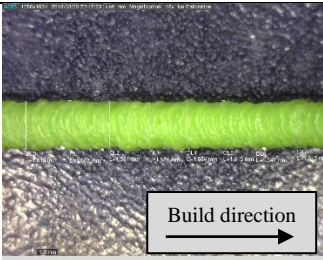
Strut diameter = 1.2 mm, Build angle = 0^0		
Set 1	Set 2	Set 3
Avg d_1 = 1.218 ± 0.014 mm	Avg d_2 = 1.225 ± 0.021 mm	Avg d_3 = 1.227 ± 0.023 mm
Avg D (1.2, 0^0) = 1.223 ± 0.020 mm		
Strut diameter = 1.2 mm, Build angle = 20^0		
Set 1	Set 2	Set 3
Avg d_1 = 1.276 ± 0.056 mm	Avg d_2 = 1.229 ± 0.110 mm	Avg d_3 = 1.218 ± 0.055 mm
Avg D (1.2, 20^0) = 1.241 ± 0.082 mm		
Strut diameter = 1.2 mm, Build angle = 35.26^0		
Set 1	Set 2	Set 3
Avg d_1 = 1.287 ± 0.068 mm	Avg d_2 = 1.212 ± 0.056 mm	Avg d_3 = 1.233 ± 0.047 mm
Avg D (1.2, 35.26^0) = 1.244 ± 0.066 mm		

32
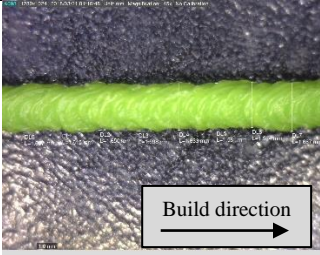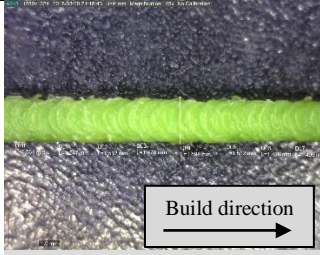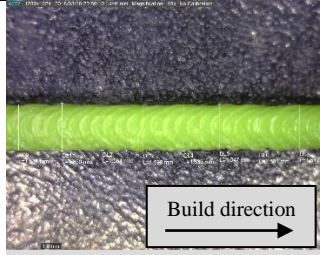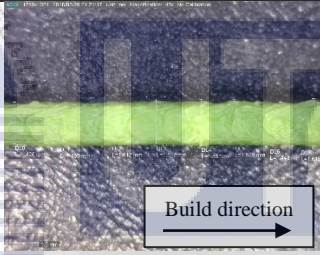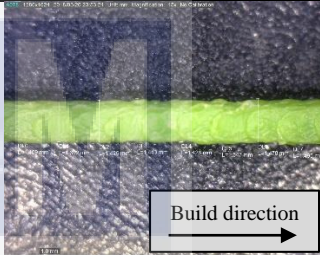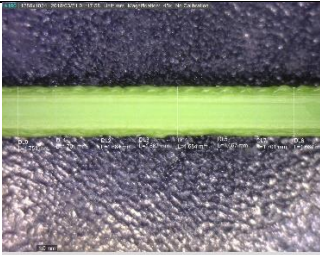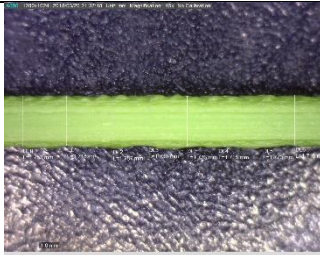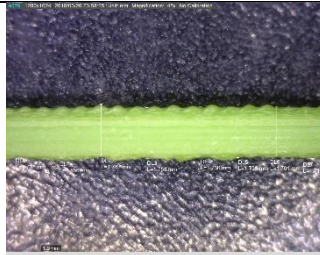
Strut diameter = 1.2 mm, Build angle = 45^0		
Set 1	Set 2	Set 3
Avg d_1 = 1.233 ± 0.052 mm	Avg d_2 = 1.199 ± 0.027 mm	Avg d_3 = 1.197 ± 0.064 mm
Avg D (1.2, 45^0) = 1.210 ± 0.053 mm		
Strut diameter = 1.2 mm, Build angle = 60^0		
Set 1	Set 2	Set 3
Avg d_1 = 1.227 ± 0.071 mm	Avg d_2 = 1.135 ± 0.055 mm	Avg d_3 = 1.221 ± 0.069 mm
Avg D (1.2, 60^0) = 1.194 ± 0.078 mm		
Strut diameter = 1.2 mm, Build angle = 80^0		
Set 1	Set 2	Set 3
Avg d_1 = 1.021 ± 0.075 mm	Avg d_2 = 0.958 ± 0.062 mm	Avg d_3 = 1.128 ± 0.045 mm
Avg D (1.2, 80^0) = 1.036 ± 0.094 mm		

Strut diameter = 1.2 mm, Build angle = 90^0		
Set 1	Set 2	Set 3
Avg d_1 = 1.055 ± 0.020 mm	Avg d_2 = 1.098 ± 0.022 mm	Avg d_3 = 1.066 ± 0.022 mm
Avg D (1.2, 90^0) = 1.073 ± 0.028 mm		

Strut diameter = 1.4 mm, Build angle = 0^0		
Set 1	Set 2	Set 3
Avg d_1 = 1.416 ± 0.026 mm	Avg d_2 = 1.427 ± 0.034 mm	Avg d_3 = 1.356 ± 0.031 mm
Avg D (1.4, 0^0) = 1.399 ± 0.044 mm		

Strut diameter = 1.4 mm, Build angle = 20^0		
Set 1	Set 2	Set 3
Avg d_1 = 1.412 ± 0.053 mm	Avg d_2 = 1.369 ± 0.103 mm	Avg d_3 = 1.453 ± 0.051 mm
Avg D (1.4, 20^0) = 1.411 ± 0.081 mm		

Strut diameter = 1.4 mm, Build angle = 35.26^0		
Set 1	**Set 2**	**Set 3**
Build direction →	Build direction →	Build direction →
Avg d_1 = 1.541 ± 0.036 mm	Avg d_2 = 1.407 ± 0.018 mm	Avg d_3 = 1.437 ± 0.071 mm
Avg D (1.4, 35.26^0) = 1.462 ± 0.074 mm		
Strut diameter = 1.4 mm, Build angle = 45^0		
Set 1	**Set 2**	**Set 3**
Build direction →	Build direction →	Build direction →
Avg d_1 = 1.427 ± 0.072 mm	Avg d_2 = 1.395 ± 0.057 mm	Avg d_3 = 1.427 ± 0.074 mm
Avg D (1.4, 45^0) = 1.416 ± 0.070 mm		
Strut diameter = 1.4 mm, Build angle = 60^0		
Set 1	**Set 2**	**Set 3**
Build direction →	Build direction →	Build direction →
Avg d_1 = 1.450 ± 0.045 mm	Avg d_2 = 1.403 ± 0.055 mm	Avg d_3 = 1.474 ± 0.051 mm
Avg D (1.4, 60^0) = 1.442 ± 0.059 mm		

Strut diameter = 1.4 mm, Build angle = 80^0		
Set 1	**Set 2**	**Set 3**
Avg d_1 = 1.259 ± 0.055 mm	Avg d_2 = 1.227 ± 0.074 mm	Avg d_3 = 1.169 ± 0.074 mm
Avg D (1.4, 80^0) = 1.218 ± 0.078 mm		
Strut diameter = 1.4 mm, Build angle = 90^0		
Set 1	**Set 2**	**Set 3**
Avg d_1 = 1.160 ± 0.022 mm	Avg d_2 = 1.319 ± 0.027 mm	Avg d_3 = 1.261 ± 0.029 mm
Avg D (1.4, 90^0) = 1.247 ± 0.071 mm		
Strut diameter = 1.6 mm, Build angle = 0^0		
Set 1	**Set 2**	**Set 3**
Avg d_1 = 1.642 ± 0.063 mm	Avg d_2 = 1.588 ± 0.044 mm	Avg d_3 = 1.470 ± 0.023 mm
Avg D (1.6, 0^0) = 1.567 ± 0.086 mm		

Strut diameter = 1.6 mm, Build angle = 20^0		
Set 1	**Set 2**	**Set 3**
Avg d_1 = 1.622 ± 0.042 mm	Avg d_2 = 1.584 ± 0.095	Avg d_3 = 1.601 ± 0.084
Avg D (1.6, 20^0) = 1.602 ± 0.079 mm		
Strut diameter = 1.6 mm, Build angle = 35.26^0		
Set 1	**Set 2**	**Set 3**
Avg d_1 = 1.627 ± 0.077 mm	Avg d_2 = 1.642 ± 0.042 mm	Avg d_3 = 1.661 ± 0.036 mm
Avg D (1.6, 35.26^0) = 1.643 ± 0.057 mm		
Strut diameter = 1.6 mm, Build angle = 45^0		
Set 1	**Set 2**	**Set 3**
Avg d_1 = 1.648 ± 0.070 mm	Avg d_2 = 1.672 ± 0.070 mm	Avg d_3 = 1.614 ± 0.043 mm
Avg D (1.6, 45^0) = 1.644 ± 0.067 mm		

Strut diameter = 1.6 mm, Build angle = 60^0		
Set 1	Set 2	Set 3
Avg d_1 = 1.622 ± 0.037 mm	Avg d_2 = 1.510 ± 0.058 mm	Avg d_3 = 1.588 ± 0.036 mm
Avg D (1.6, 60^0) = 1.574 ± 0.065 mm		

Strut diameter = 1.6 mm, Build angle = 80^0		
Set 1	Set 2	Set 3
Avg d_1 = 1.534 ± 0.083 mm	Avg d_2 = 1.519 ± 0.061 mm	Avg d_3 = 1.452 ± 0.048 mm
Avg D (1.6, 80^0) = 1.502 ± 0.075 mm		

Strut diameter = 1.6 mm, Build angle = 90^0		
Set 1	Set 2	Set 3
Avg d_1 = 1.691 ± 0.028 mm	Avg d_2 = 1.742 ± 0.025	Avg d_3 = 1.750 ± 0.052 mm
Avg D (1.6, 90^0) = 1.728 ± 0.045 mm		

In calculating the average diameter (Avg D), the Equation 4.1 is applied. In this equation, x represents the reading of measured diameter while N is the number of readings in a single strut.

$$Avg\ D = \frac{\sum x}{N} \qquad [4.1]$$

Next, Equation 4.2 is applied to calculate the standard deviation, σ. The x is the reading of measured diameter, $\bar{x}$ is the mean or also known as average data, and N is the number of readings in a single strut.

$$\sigma = \frac{\sqrt{\sum(x-\bar{x})^2}}{N} \qquad [4.2]$$

Moreover, to calculate percentage difference (%), the Equation 4.3 is applied. The x_e represents the experimental value which is the reading of measured diameter. The x_a is the actual value which is the designed diameter of a single strut.

$$Percentage\ different\ (\%) = \frac{x_e - x_a}{x_a} \times 100\% \qquad [4.3]$$

Hence, all the calculated values of average diameter (Avg D) and standard deviation (σ) for each single strut are recorded in the Table 4.4.1 as well. On the other hand, the values of calculated percentage difference (%) are presented in Table 4.4.2.

Table 4.4.2: The percentage difference of each single strut.

Build angle (^{o})	Strut diameter					
	1.2mm		1.4mm		1.6mm	
	Average D (mm)	Percentage difference (%)	Average D (mm)	Percentage difference (%)	Average D (mm)	Percentage difference (%)
0	1.223 ± 0.020	1.92	1.399 ± 0.044	-0.07	1.567 ± 0.086	-2.06
20	1.241 ± 0.082	3.42	1.411 ± 0.081	0.79	1.602 ± 0.079	0.13
35.26	1.244 ± 0.066	3.67	1.462 ± 0.074	4.43	1.643 ± 0.057	2.69
45	1.210 ± 0.053	0.83	1.416 ± 0.070	1.14	1.644 ± 0.067	2.75
60	1.194 ± 0.078	-0.50	1.442 ± 0.059	3.00	1.574 ± 0.065	-1.63
80	1.036 ± 0.094	-13.67	1.218 ± 0.078	-13.00	1.502 ± 0.075	-6.13
90	1.073 ± 0.028	-10.58	1.247 ± 0.071	-10.93	1.728 ± 0.045	8.00

Table 4.4.2 shows the percentage difference between measured diameter and designed diameter of each single strut. The single strut with 1.4mm diameter and 0° build angle has the lowest of percentage difference which is 0.07%. On the other hand, the single strut with 1.2mm diameter and 80° build angle has the highest of percentage difference which is 13.67%. In overall, all the single struts have the accuracy of more than 86% based on the readings of measured diameter. Hence, a graph of strut diameter versus build angle is plotted and shown in Figure 4.4.3. There are three series in the graph which represent the diameter of 1.2mm, 1.4mm and 1.6mm respectively. Based on the graph, the 80° and 90° build angles have larger difference to the designed diameter as compared to other build angles.
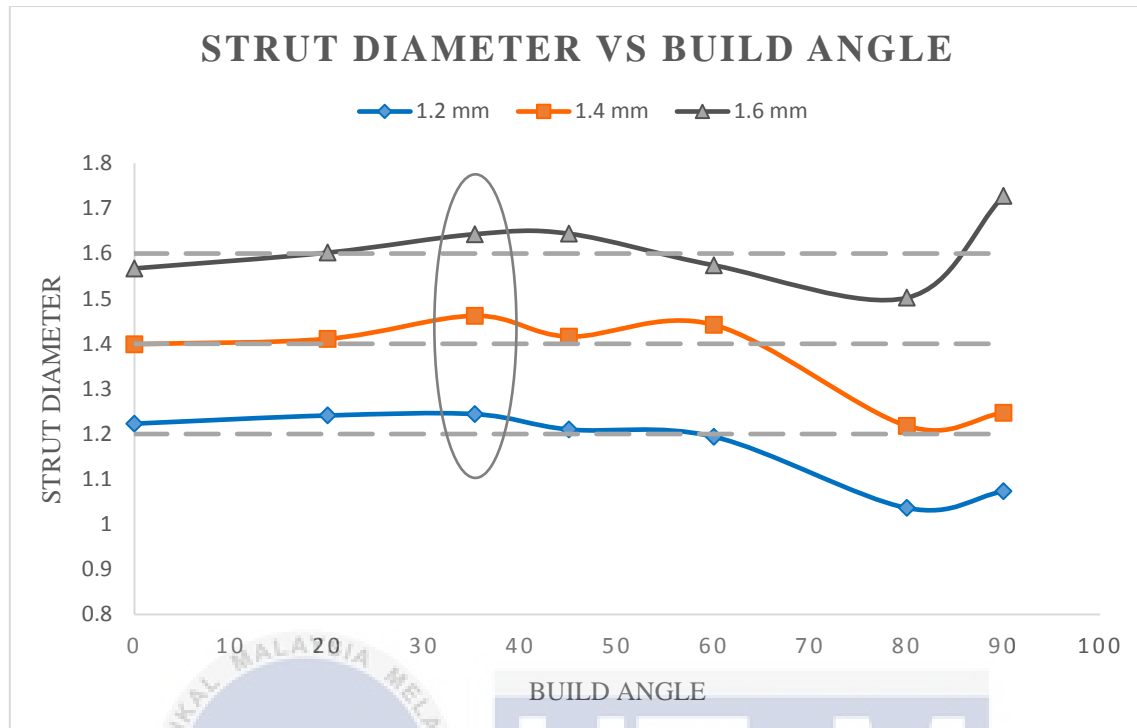
Figure 4.4.3: Graph of strut diameter versus build angle.

Among these single struts, the single struts with 35.26º build angle are given more focused as the 35.26º represents the angle of the strut to the surface in BCC structure (Azmi et al., 2017). As they are mimicking the struts in BCC arrangement, when the BCC lattice structure is fabricated, the diameter of struts in BCC lattice configuration will be more or less about the same with that single strut fabricated at 35.26º build angle. Hence, the surface roughness analysis is conducted for the selected single struts with 35.26º build angle.

Table 4.4.3: The selected struts for surface roughness analysis.

	Struts with 35.26° build angle		
Strut diameter category	1.2mm	1.4mm	1.6mm
Average diameter, Avg D (mm)	1.244	1.462	1.643
Selected strut diameter (mm)	1.233 (Set 3)	1.437 (Set 3)	1.642 (Set 2)

Table 4.4.3 shows the only three single struts with 35.26° build angle are selected for surface roughness analysis. These single struts are chosen because they have the nearest value to the average diameter value. Therefore, these three single struts are analysed on their surface roughness using the Dino-Lite Pro. In this process, the magnification scale of 55x is used for analysing these specimens. Moreover, eights peaks and eight valleys are selected in order to obtain the R_a (Roughness Average) value. The applied equation of R_a is shown in Equation 4.4 where l is the evaluation length and $Z(x)$ is the profile height function. Figures 4.4.4, 4.4.5 and 4.4.6 show the image captured from the Dino-Lite software for surface roughness analysis.

$$R_a = \frac{1}{l}\int_0^l |Z(x)|dx \qquad\qquad [4.4]$$
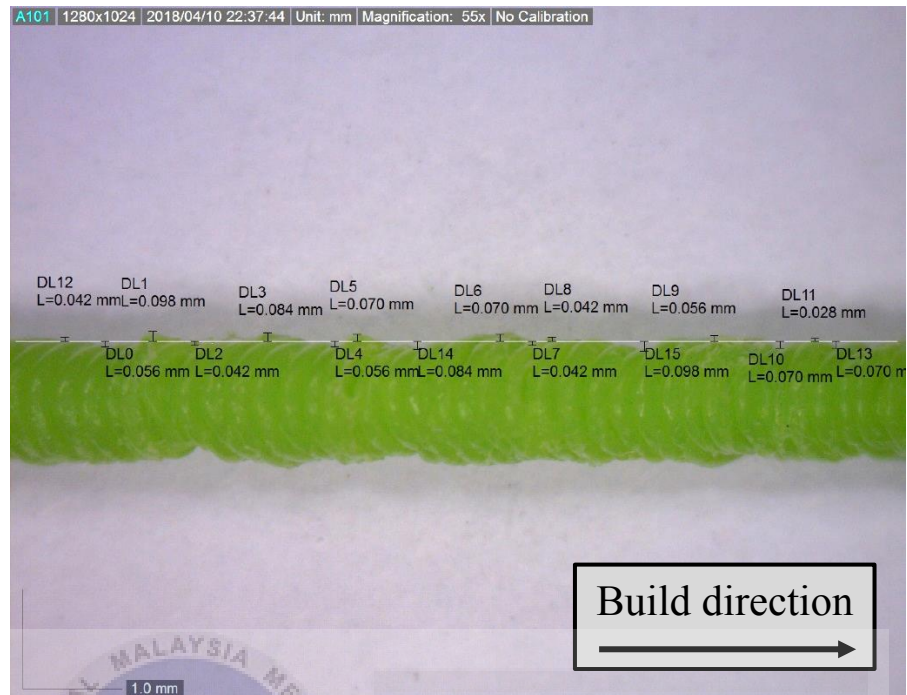
Figure 4.4.4: Surface roughness analysis for 1.2mm strut diameter using Dino-Lite Pro.

Figure 4.4.5: Surface roughness analysis for 1.4mm strut diameter using Dino-Lite Pro.
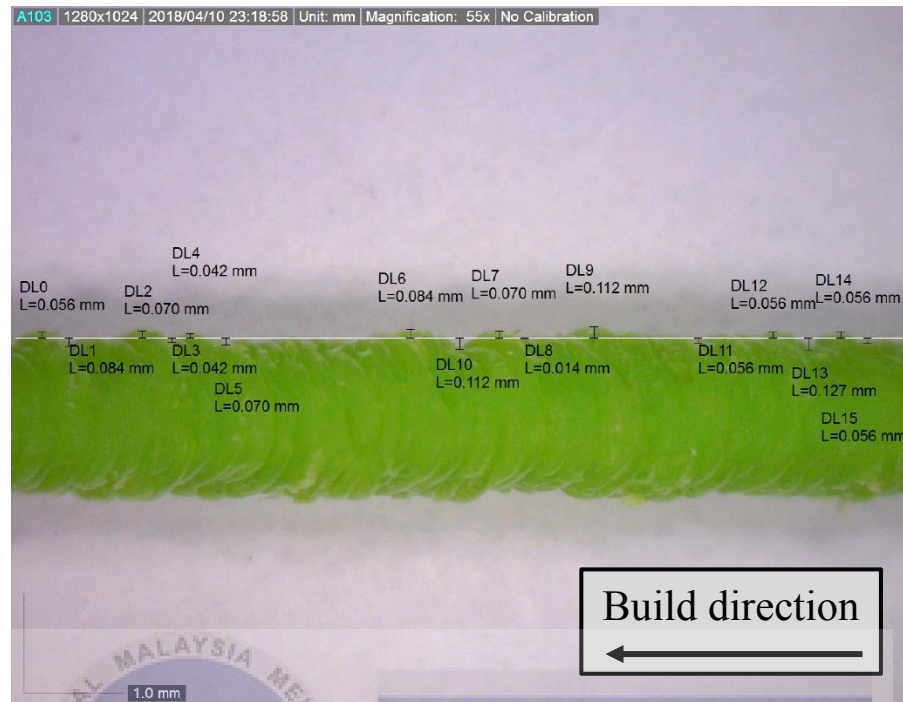
Figure 4.4.6: Surface roughness analysis for 1.6mm strut diameter using Dino-Lite Pro.

Apart from that, 3D non-contact profilometer is used for these three single struts to analyse their surface roughness as well. The selected single strut is observed under the microscope and also viewed in the WinRoof software. The results obtained from the WinRoof software include the 3D profile of the selected single strut, a graph of its height versus its length and the roughness (R_a) value. These results presented in Excel file for each single strut are shown in Figures 4.4.7, 4.4.8 and 4.4.9.

44

	Name	Height [um]	Width1 [u	Area [um	Diagonal	Surface L	Roughne	Roughne	RoughnessRzjis
Height	72.6942	um							
Width	5.7238	um							
Area	223.4428	um^2							
Diagonal	72.9192	um							
Surface Length	5.7719	um							
Roughness Ra	22.8935	um							
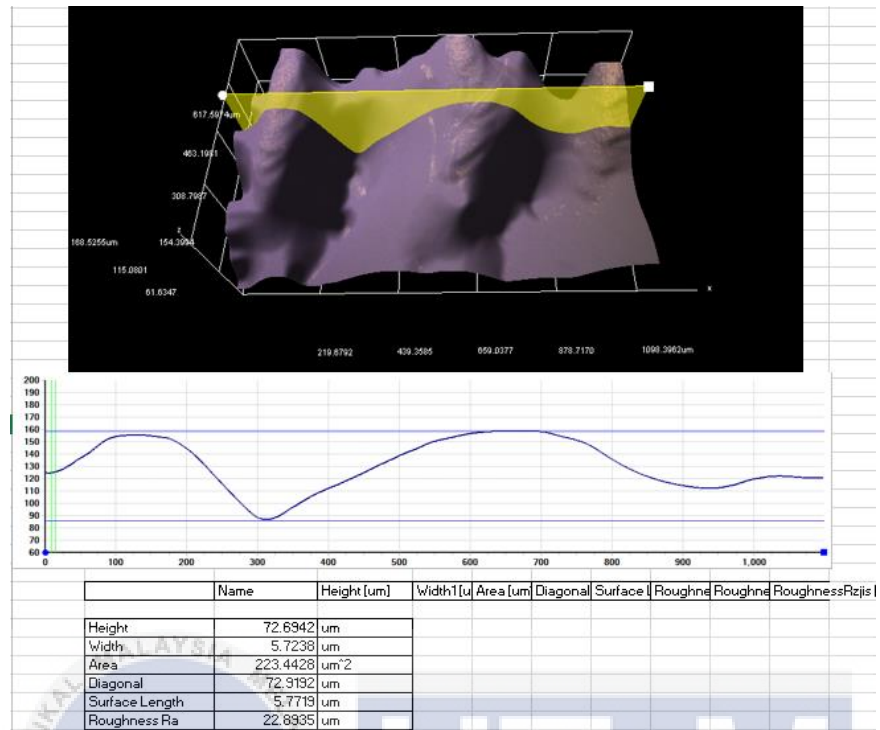
Figure 4.4.7: Surface roughness analysis for 1.2mm strut diameter using 3D non-contact profilometer.

	Name	Height [um]	Width1 [u	Area [um	Diagonal	Surface	Roughne	Roughne	RoughnessRzjis [
Height	140.3608	um							
Width	5.7238	um							
Area	677.4352	um^2							
Diagonal	140.4774	um							
Surface Length	5.7261	um							
Roughness Ra	33.2735	um							
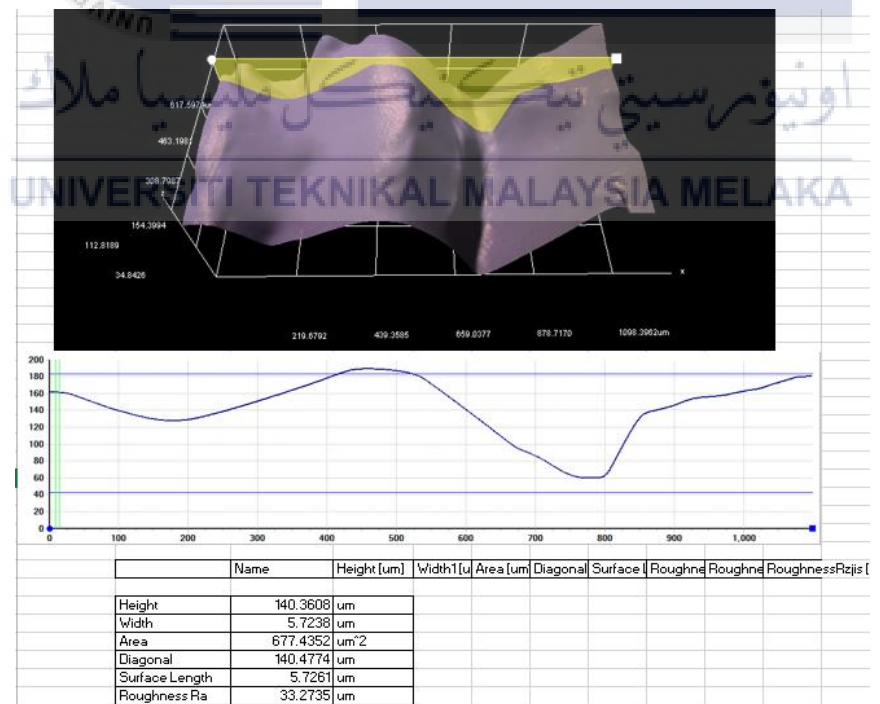
Figure 4.4.8: Surface roughness analysis for 1.4mm strut diameter using 3D non-contact profilometer.
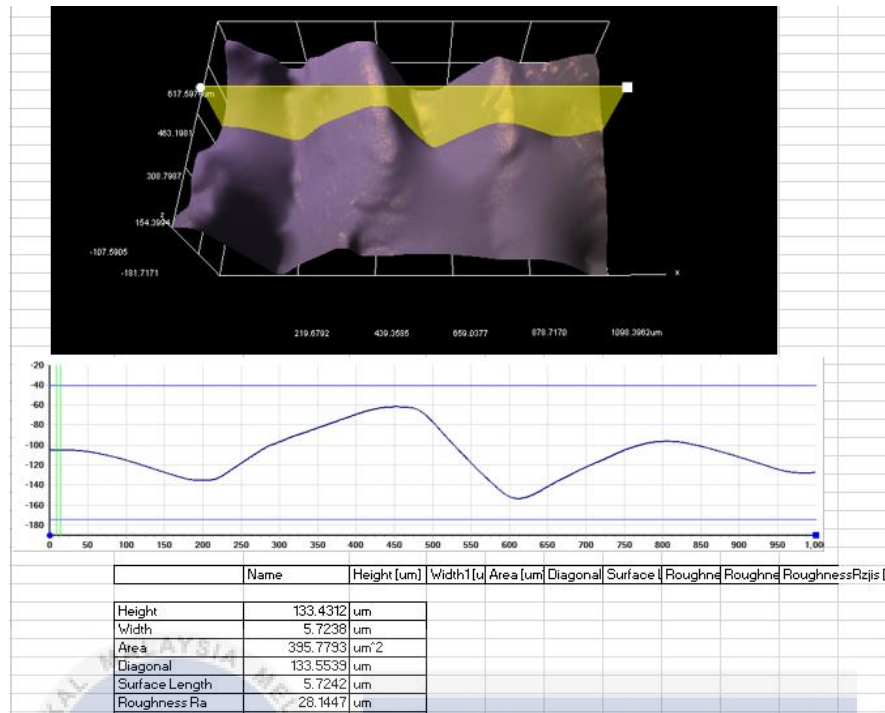
Figure 4.4.9: Surface roughness analysis for 1.6mm strut diameter using 3D non-contact profilometer.

Table 4.4.4: Tabulation of R_a values.

Strut diameter (mm)	Surface roughness, R_a (µm)	
	Theoretical	Profilometer
1.2	63	22.89
1.4	75.38	33.27
1.6	69.19	28.14

By gathering the both R_a values from two different surface roughness analysis, those R_a values for three selected singles struts are tabulated in the Table 4.4.4. Based on the results obtained, the single strut with 1.2mm diameter for 35.26° build angles has the lowest R_a value,

46

then follow by strut with 1.6mm diameter and the strut with 1.4mm diameter has the highest R_a value. The lowest R_a value is 63µm in theoretically and also 22.89µm when examined using 3D non-contact profilometer. The theoretically value is obtained by applying the Equation 4.4 to calculate the R_a value after determined the peak values and valley values on the surface of single strut in the Dino-Lite software.

However, both R_a values are different as the evaluated length of single strut is different in both analysis process. Based on the Figure 4.4.10, the evaluated length of single strut in Dino-Lite Pro analysis is longer as compared to 3D non-contact profilometer. As the evaluated length of single strut in Dino-Lite Pro analysis is longer, more peak values and valley values are determined to calculate the R_a value. Hence, the R_a values in theoretically which are obtained in the Dino-Lite Pro analysis are more accurate as more peak values and valley values are considered into the calculation.
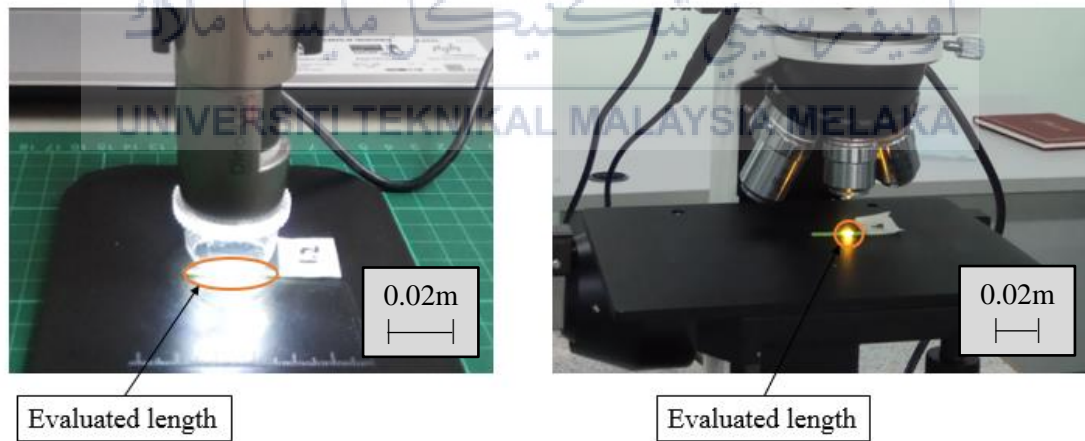
Figure 4.4.10: Dino-Lite Pro analysis and 3D non-contact profilometer analysis.

Furthermore, a graph of surface roughness versus strut diameter is constructed for both Dino-Lite Pro analysis and 3D non-contact profilometer analysis as shown on Figure 4.4.11. Based on this graph, the struts with 1.2 and 1.6mm diameter have lower R_a value while the strut with 1.4mm diameter has higher R_a value. Since the layer resolution for these single struts are the same which is 200μm, however the nozzle diameter is another factor that can affect the dimensions of printed part (Reyes-Rodríguez et al., 2017). The nozzle diameter of CubePro 3D printer is 0.4mm. As the 1.2 and 1.6 are the multiple of 0.4, hence the struts with 1.2mm and 1.6mm diameter have better accuracy in dimensions.
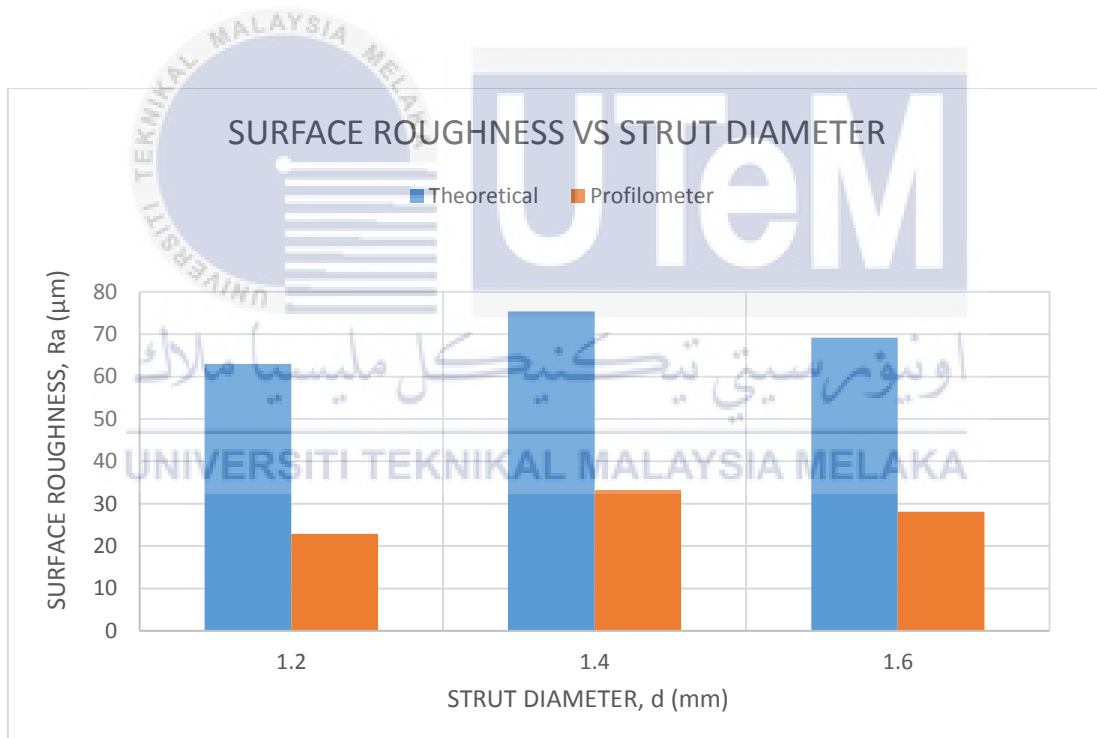
Figure 4.4.11: Graph of surface roughness versus strut diameter.

4.5   Summary of Chapter 4

In conclusion, three sets of designed 21 single struts can be printed using CubePro. In order to fabricate successfully the single struts, they have to be designed with their suitable supports. Next, the single struts are analysed on their diameter using Dino-Lite Pro and the results obtained are tabulated. Apart from that, the selected single struts are then analysed on their surface roughness using Dino-Lite Pro and 3D non-contact profilometer. The results obtained from both equipment are tabulated and a graph of surface roughness versus strut diameter is constructed.

CHAPTER 5

CONCLUSION AND RECOMMENDATION

5.1   Conclusion

This study is conducted to analyse the formation of fabricated single struts with different diameter sizes and build angles using CubePro 3D printer. The chosen diameters of single struts are 1.2mm, 1.4mm and 1.6mm while the build angles are set as 0°, 20°, 35.26^o, 45°, 60°, 80° and 90° from a vertical line. The background of this study is reviewed to gain the relevant knowledge and scientific theories. The previous researches are studied to learn the different methods in producing lattice-structure materials and single struts.

In methodology, the single struts are designed using a CAD software which is CATIA. Next, the designed single struts are fabricated using CubePro 3D printer. The fabricated single struts are then analysed on their diameter by using Dino-Lite Pro. Moreover, the selected struts with 35.26^o build angle are analysed on their surface roughness by using Dino-Lite Pro and 3D non-contact profilometer. By following workflow chart, the results are obtained and discussed in this study.

Three sets of 21 specimens are fabricated using CubePro 3D printer successfully. For diameter analysis, a graph of strut diameter versus build angle is plotted. Based on the graph, the 80° and 90° build angles have larger difference to the designed diameter as compared to other build angles. However, all the single struts still have the accuracy of more than 86% based on the readings of measured diameter. For surface roughness analysis, a graph of surface

roughness versus strut diameter is constructed for both Dino-Lite Pro analysis and 3D non-contact profilometer analysis. Based on the results obtained, the single strut with 1.2mm diameter for 35.26º build angles has the lowest R_a value, then follow by strut with 1.6mm diameter and the strut with 1.4mm diameter has the highest R_a value. This is due to the 0.4mm nozzle diameter of CubePro 3D printer as a factor to affect the dimensions of printed part.

5.2   Recommedation

For the future study, physical test on individual strut and also struts arranged in lattice structure can be conducted. Hence, a comparison can be made between both results obtained from the physical tests. By making this comparison between individual strut and struts arranged in lattice structure, the difference in both performances can be studied and some improvements also can be made in order to enhance the both performances.

REFERENCES

3D Systems Inc. (2015). CubePro Prosumer 3D printer - User Guide - Original Instructions. *3D Systems, Inc.*, (September), 1–86. https://doi.org/10.4337/9781782545583.00006 [Assesed on 25 Oct. 2017].

3dsystems.com. (2017). CubePro 3D Printer - Technical Specifications - 3D Systems. https://www.3dsystems.com/shop/cubepro/techspecs [Accessed 25 Oct. 2017].

Azmi, M. S., Ismail, R., Hasan, R., & Alkahari, M., R. (2017). Study on dimensional accuracy of lattice structure bar using FDM additive manufacturing. *Proceedings of Mechanical Engineering Research Day 2017*, pp. 397-398.

Dong, G., Wijaya, G., Tang, Y., & Zhao, Y. F. (2018). Optimizing process parameters of fused deposition modeling by Taguchi method for the fabrication of lattice structures. *Additive Manufacturing*, 19, 62–72.

Doyoyo, M. and Hu, J. (2006). Multi-axial failure of metallic strut-lattice materials composed of short and slender struts. *International Journal of Solids and Structures*, 43(20), pp.6115-6139.

Gebhardt, A. (2003). Rapid prototyping. Munich: Hanser Publishers.

Kessler, J., Bâlc, N., Gebhardt, A., & Abbas, K. (2016). Basic Research on Lattice Structures Focused on the strut shape and welding beads. *Physics Procedia*, 83, 833–838.

Rashed, M., Ashraf, M., Mines, R. and Hazell, P. (2016). Metallic microlattice materials: A current state of the art on manufacturing, mechanical properties and applications. *Materials & Design*, 95, pp.518-533.

Reinhart, G., Teufelhart, S., & Riss, F. (2012). Investigation of the Geometry-dependent Anisotropic Material Behavior of Filigree Struts in ALM-produced Lattice Structures. *Physics Procedia*, 39, 471–479.

Reinhart, G. and Teufelhart, S. (2013). Optimization of Mechanical Loaded Lattice Structures by Orientating their Struts Along the Flux of Force. *Procedia CIRP*, 12, pp.175-180.

Reyes-Rodríguez, A., Dorado-Vicente, R., & Mayor-Vicario, R. (2017). Dimensional and form errors of PC parts printed via Fused Deposition Modelling. *Procedia Manufacturing*, 13, 880-887.

Syam, W., Jianwei, W., Zhao, B., Maskery, I., Elmadih, W. and Leach, R. (2017). Design and analysis of strut-based lattice structures for vibration isolation. *Precision Engineering*, 24, 510-523.

Tang, Y., Dong, G., Zhou, Q., & Zhao, Y. (2017). Lattice Structure Design and Optimization With Additive Manufacturing Constraints. *IEEE Transactions On Automation Science And Engineering*, 1-17.

Tsopanos, S., Mines, R.A.W., McKown, S., Shen, Y., Cantwell, W. J., Brooks, W., & Sutcliffe, C. J. (2010). The influence of processing parameters on the mechanical properties of selectively laser melted stainless steel microlatticestructures. *Journal of Manufacturing Science and Engineering*, 132: 041011-1 - 140111-12.

Figure A1: The dimension drawing of single struts with 0º using CATIA.

Fugure A2: The dimension drawing of single struts with 20° using CATIA.

Figure A3: The dimension drawing of single struts with 35.26º using CATIA.

Figure A4: The dimension drawing of single struts with 45° using CATIA.

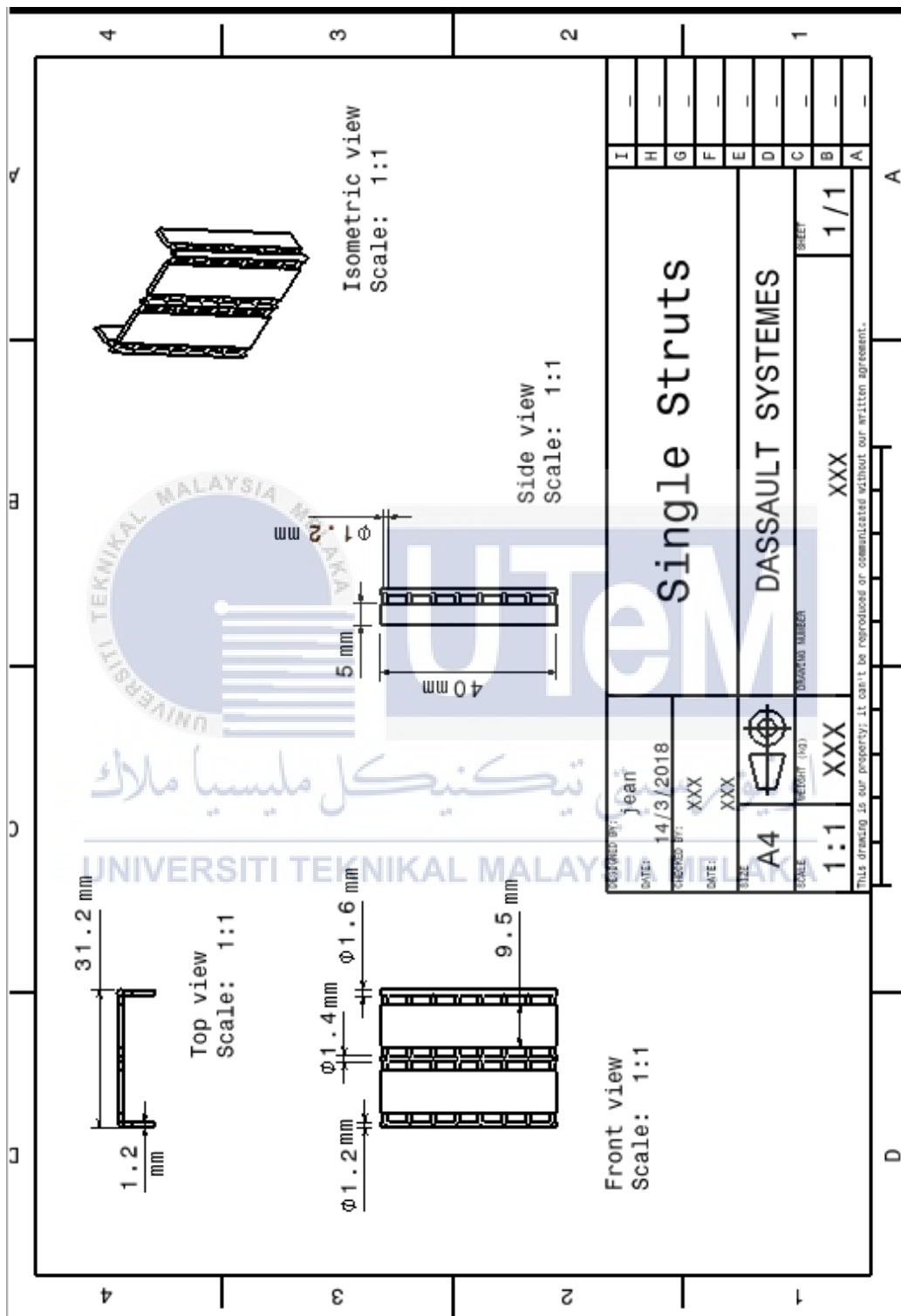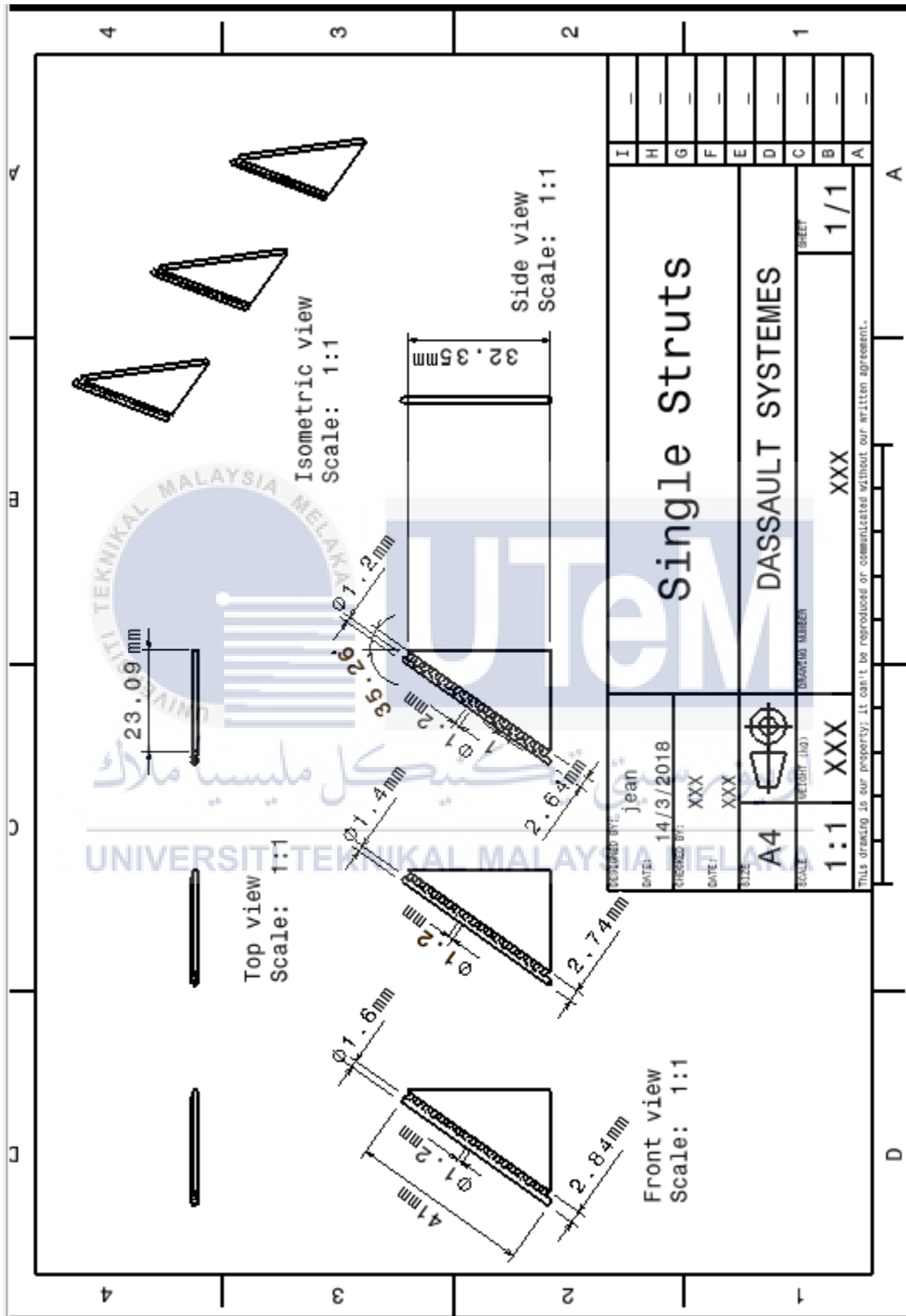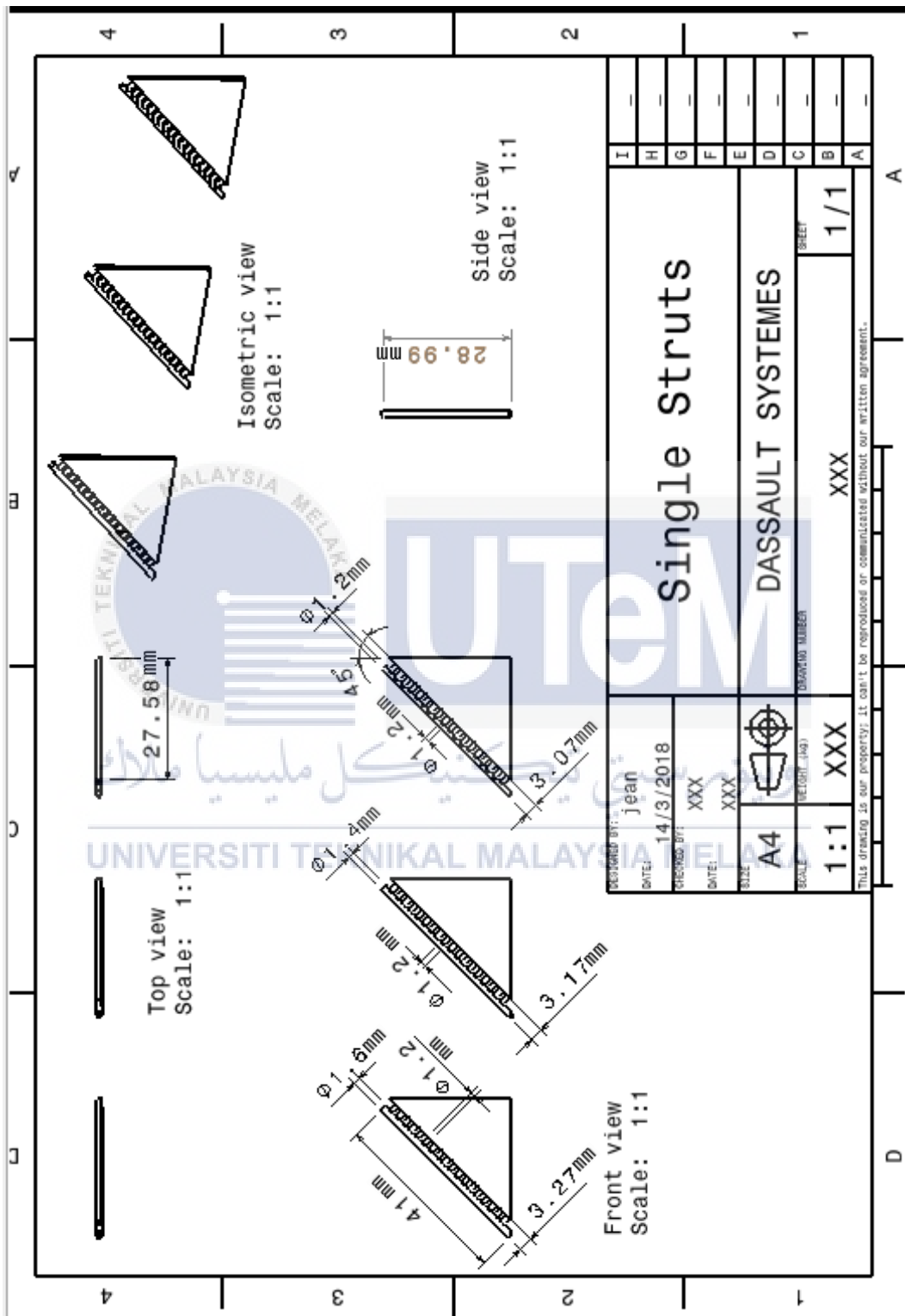Figure A5: The dimension drawing of single struts with 60° using CATIA.

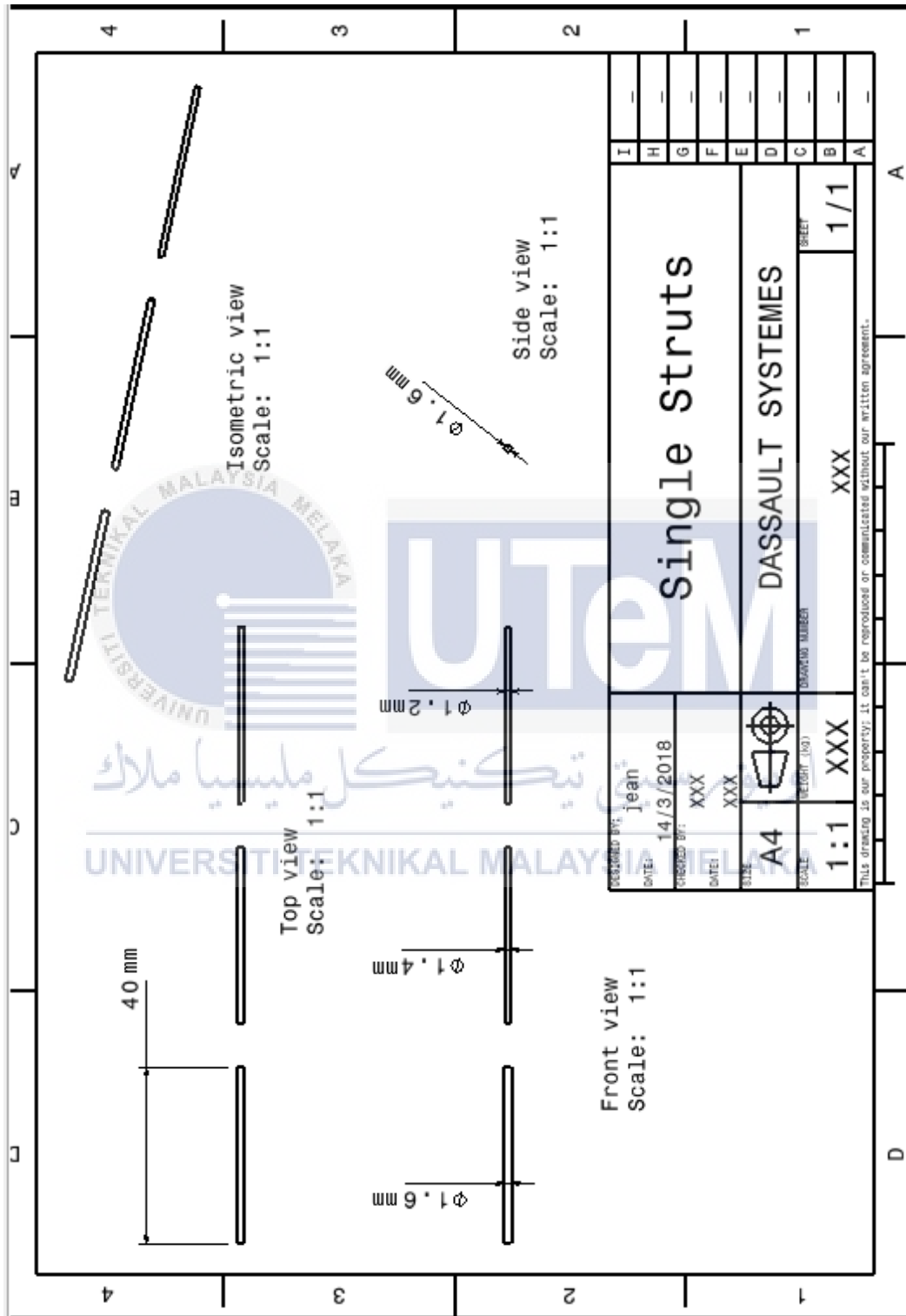Figure A6: The dimension drawing of single struts with 80º using CATIA.

Figure A7: The dimension drawing of single struts with 90º using CATIA.
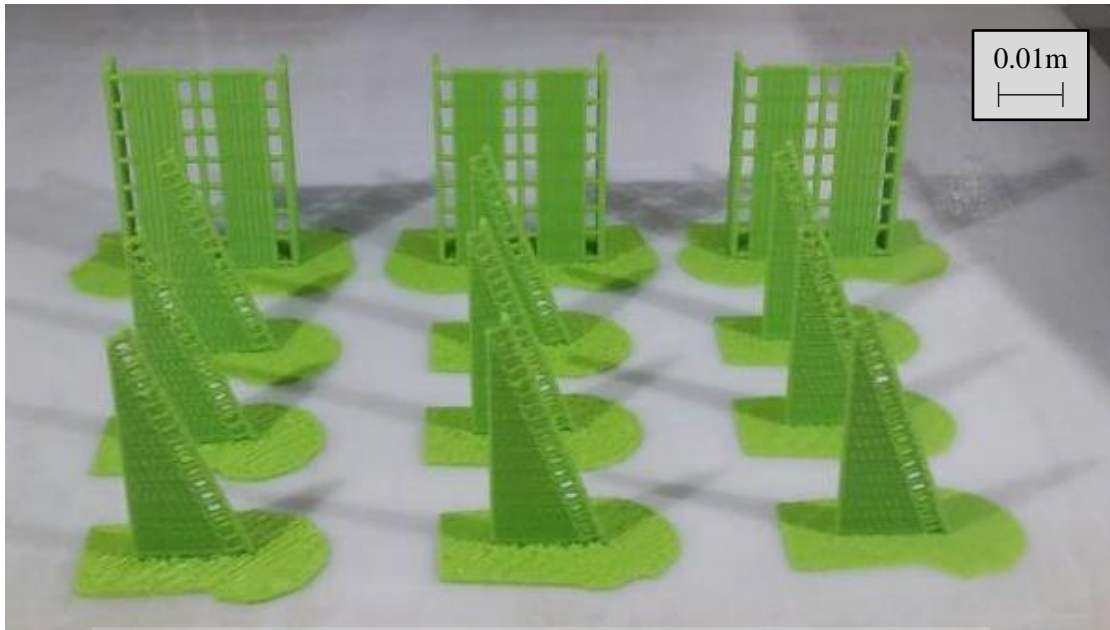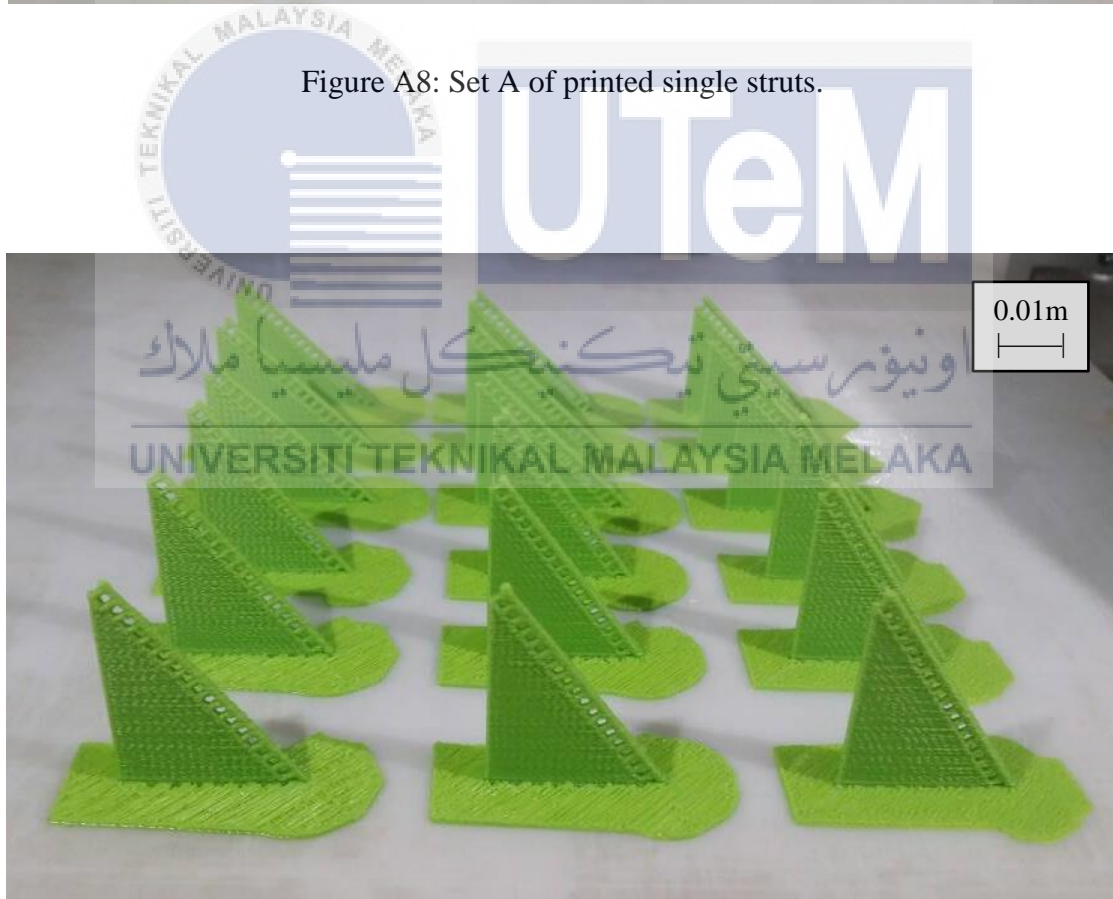
Figure A8: Set A of printed single struts.

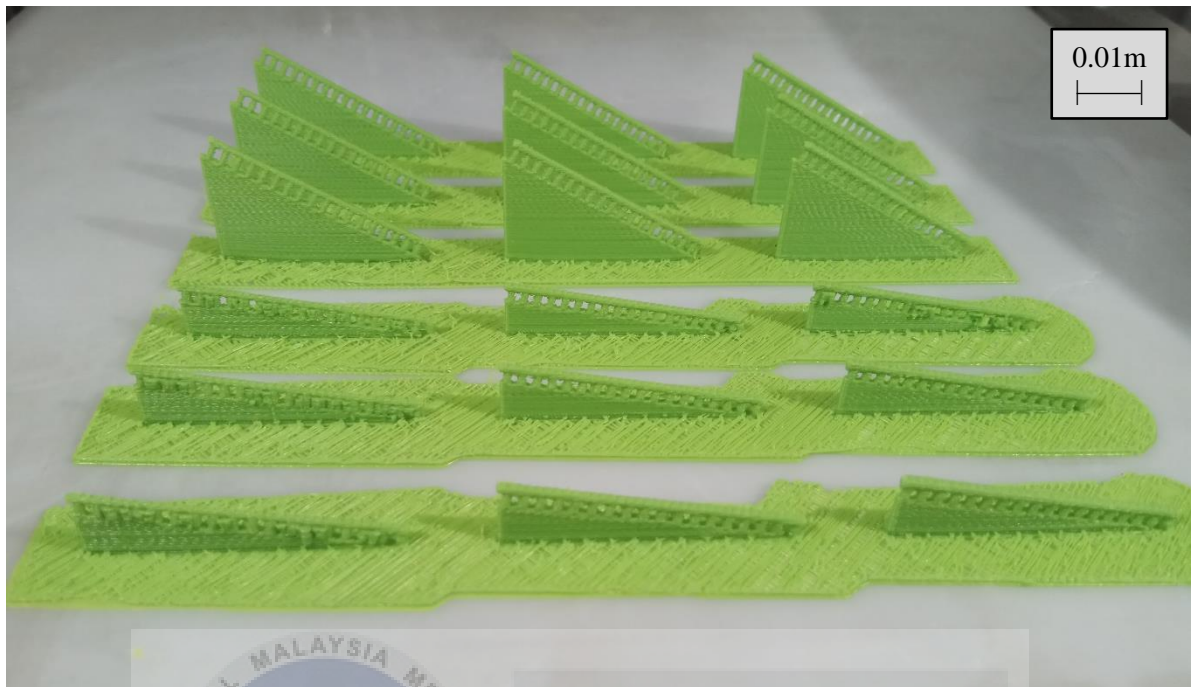Figure A9: Set B of printed single struts.

Figure A10: Set C of printed single struts.

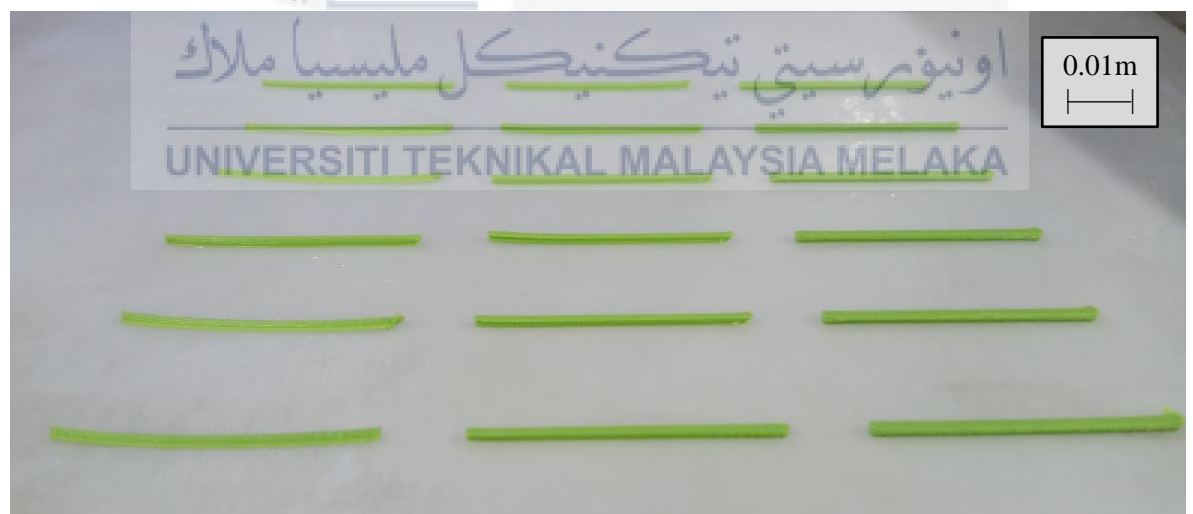Figure A11: Set D of printed single struts.

set 1

	1,2, 0	1,2, 20	1,2, 35	1,2, 45	1,2, 60	1,2, 80	1,2, 90		1,4, 0	1,4, 20	1,4, 35	1,4, 45	1,4, 60	1,4, 80	1,4, 90		1,6, 0	1,6, 20	1,6, 35	1,6, 45	1,6, 60	1,6, 80	1,6, 90
	1.22	1.289	1.323	1.237	1.169	1.083	1.031		1.426	1.34	1.564	1.495	1.409	1.237	1.151		1.667	1.615	1.598	1.753	1.667	1.495	1.753
	1.22	1.323	1.409	1.251	1.358	1.014	1.048		1.409	1.461	1.581	1.512	1.426	1.186	1.186		1.718	1.701	1.633	1.633	1.615	1.529	1.701
	1.203	1.289	1.254	1.22	1.186	1.083	1.031		1.443	1.478	1.512	1.323	1.547	1.254	1.151		1.684	1.598	1.581	1.753	1.65	1.615	1.684
	1.203	1.375	1.203	1.323	1.186	0.859	1.048		1.392	1.409	1.547	1.461	1.426	1.306	1.117		1.667	1.633	1.65	1.598	1.598	1.529	1.667
	1.203	1.289	1.306	1.289	1.323	1.048	1.048		1.375	1.409	1.598	1.34	1.495	1.186	1.151		1.564	1.615	1.65	1.564	1.633	1.392	1.684
	1.22	1.203	1.323	1.203	1.203	0.962	1.065		1.392	1.358	1.512	1.358	1.443	1.358	1.186		1.581	1.615	1.65	1.684	1.581	1.547	1.667
	1.237	1.203	1.289	1.169	1.151	1.014	1.083		1.443	1.358	1.495	1.495	1.409	1.254	1.169		1.701	1.547	1.77	1.581	1.564	1.478	1.701
	1.237	1.237	1.186	1.169	1.237	1.1	1.083		1.443	1.478	1.512	1.426	1.443	1.289	1.169		1.547	1.65	1.478	1.615	1.667	1.684	1.667
Avg	1.218	1.276	1.287	1.233	1.227	1.021	1.055		1.416	1.412	1.541	1.427	1.45	1.259	1.16		1.642	1.622	1.627	1.648	1.622	1.534	1.691
Std dvt	0.014	0.056	0.068	0.052	0.071	0.075	0.02		0.026	0.053	0.036	0.072	0.045	0.055	0.022		0.063	0.042	0.077	0.07	0.037	0.083	0.028

Figure A12: The readings of measured diameter for each single strut in Set 1.

set 2

	1,2, 0	1,2, 20	1,2, 35	1,2, 45	1,2, 60	1,2, 80	1,2, 90		1,4, 0	1,4, 20	1,4, 35	1,4, 45	1,4, 60	1,4, 80	1,4, 90		1,6, 0	1,6, 20	1,6, 35	1,6, 45	1,6, 60	1,6, 80	1,6, 90
	1.203	1.203	1.203	1.22	1.083	0.997	1.117		1.426	1.392	1.392	1.461	1.461	1.254	1.289		1.547	1.461	1.598	1.65	1.564	1.426	1.753
	1.22	1.375	1.186	1.203	1.186	1.014	1.134		1.409	1.237	1.409	1.409	1.426	1.134	1.306		1.633	1.753	1.701	1.701	1.547	1.495	1.718
	1.254	1.1	1.272	1.186	1.117	0.876	1.117		1.409	1.478	1.426	1.409	1.443	1.254	1.306		1.65	1.615	1.684	1.77	1.598	1.512	1.787
	1.22	1.151	1.254	1.254	1.169	0.859	1.083		1.443	1.426	1.392	1.461	1.461	1.186	1.289		1.547	1.512	1.581	1.633	1.512	1.547	1.736
	1.254	1.358	1.306	1.186	1.203	1.031	1.1		1.495	1.289	1.409	1.392	1.375	1.323	1.323		1.529	1.547	1.633	1.787	1.426	1.581	1.736
	1.237	1.272	1.169	1.169	1.031	0.928	1.083		1.409	1.272	1.443	1.272	1.375	1.34	1.323		1.633	1.478	1.633	1.615	1.512	1.529	1.718
	1.203	1.065	1.169	1.203	1.117	1.014	1.083		1.375	1.547	1.392	1.358	1.392	1.151	1.34		1.581	1.667	1.615	1.581	1.426	1.443	1.77
	1.203	1.306	1.134	1.169	1.169	0.945	1.065		1.443	1.306	1.392	1.392	1.289	1.169	1.375		1.581	1.633	1.684	1.633	1.495	1.615	1.718
Avg	1.225	1.229	1.212	1.199	1.135	0.958	1.098		1.427	1.369	1.407	1.395	1.403	1.227	1.319		1.588	1.584	1.642	1.672	1.51	1.519	1.742
Std dvt	0.021	0.11	0.056	0.027	0.055	0.062	0.022		0.034	0.103	0.018	0.057	0.055	0.074	0.027		0.044	0.095	0.042	0.07	0.058	0.061	0.025

Figure A13: The readings of measured diameter for each single strut in Set 2.

set 3

	1,2, 0	1,2, 20	1,2, 35	1,2, 45	1,2, 60	1,2, 80	1,2, 90		1,4, 0	1,4, 20	1,4, 35	1,4, 45	1,4, 60	1,4, 80	1,4, 90		1,6, 0	1,6, 20	1,6, 35	1,6, 45	1,6, 60	1,6, 80	1,6, 90
	1.254	1.22	1.289	1.323	1.323	1.065	1.083		1.358	1.478	1.375	1.426	1.461	1.065	1.289		1.461	1.443	1.65	1.615	1.581	1.409	1.701
	1.254	1.169	1.306	1.237	1.169	1.083	1.048		1.358	1.392	1.512	1.529	1.547	1.169	1.272		1.512	1.667	1.684	1.65	1.65	1.392	1.865
	1.22	1.169	1.22	1.134	1.306	1.117	1.065		1.409	1.426	1.443	1.289	1.426	1.117	1.306		1.478	1.529	1.667	1.581	1.564	1.426	1.787
	1.22	1.34	1.203	1.203	1.203	1.151	1.1		1.375	1.461	1.409	1.426	1.443	1.186	1.254		1.478	1.615	1.633	1.581	1.598	1.443	1.753
	1.203	1.203	1.254	1.22	1.203	1.117	1.065		1.34	1.547	1.426	1.461	1.443	1.289	1.254		1.426	1.615	1.736	1.684	1.633	1.426	1.736
	1.254	1.22	1.151	1.134	1.272	1.151	1.083		1.306	1.495	1.306	1.34	1.409	1.117	1.22		1.461	1.547	1.615	1.615	1.547	1.547	1.736
	1.203	1.169	1.22	1.203	1.169	1.117	1.031		1.375	1.392	1.529	1.495	1.512	1.134	1.272		1.461	1.718	1.667	1.547	1.581	1.478	1.701
	1.203	1.254	1.22	1.117	1.117	1.22	1.048		1.323	1.426	1.495	1.443	1.547	1.272	1.22		1.478	1.667	1.633	1.615	1.547	1.495	1.718
Sum																							
Avg	1.227	1.218	1.233	1.197	1.221	1.128	1.066		1.356	1.453	1.437	1.427	1.474	1.169	1.261		1.47	1.601	1.661	1.614	1.588	1.452	1.75
Std dvt	0.023	0.055	0.047	0.064	0.069	0.045	0.022		0.031	0.051	0.071	0.074	0.051	0.074	0.029		0.023	0.084	0.036	0.043	0.036	0.048	0.052

Figure A14: The readings of measured diameter for each single strut in Set 3.

	1.2 mm				1.6 mm			
peak	valley	avg	RA	peak	valley	avg	RA
98	98	98	63 µm	112	127	119.5	69.1875 µm
84	84	84		84	112	98	
70	70	70		70	84	77	
70	70	70		70	70	70	
56	56	56		56	56	56	
42	56	49		56	56	56	
42	42	42		56	42	49	
28	42	35		42	14	28	

	1.4 mm		
peak	valley	avg	RA
141	127	134	75.375 µm
112	112	112	
98	98	98	
84	84	84	
28	84	56	
28	70	49	
28	42	35	
28	42	35	

Figure A15: The readings of peak values and valley values for the selected single strut with 35.26º build angle.